



HAL
open science

Capillary electrophoresis for enzyme-based studies: Applications to lipases and kinases

Ghassan Al Hamoui Dit Banni, Reine Nehmé

► To cite this version:

Ghassan Al Hamoui Dit Banni, Reine Nehmé. Capillary electrophoresis for enzyme-based studies: Applications to lipases and kinases. *Journal of Chromatography A*, 2022, 1661, pp.462687. <10.1016/j.chroma.2021.462687>. <hal-03706495>

HAL Id: hal-03706495

<https://univ-orleans.hal.science/hal-03706495v1>

Submitted on 5 Jan 2024

HAL is a multi-disciplinary open access archive for the deposit and dissemination of scientific research documents, whether they are published or not. The documents may come from teaching and research institutions in France or abroad, or from public or private research centers.

L'archive ouverte pluridisciplinaire HAL, est destinée au dépôt et à la diffusion de documents scientifiques de niveau recherche, publiés ou non, émanant des établissements d'enseignement et de recherche français ou étrangers, des laboratoires publics ou privés.



Distributed under a Creative Commons CC BY-NC 4.0 - Attribution - Non-commercial use - International License

33	Outline	
34	1. Introduction.....	3
35	2. CE-based lipase assays.....	5
36	3. CE-based nucleoside kinase assays.....	16
37	4. Conclusion.....	23
38	5. Declarations	23
39	6. References.....	24
40		

41 **1. Introduction**

42 Enzyme catalyzed reactions and abnormal perturbations in their function are implicated, either
43 directly or indirectly, in the development of several disorders such as infections [1,2], cancers
44 [3,4], obesity [5] or skin aging [6]. Assaying the catalytic activity of enzymes expedites the
45 elaboration of the molecular mechanisms through which enzymes function and influence the
46 development of diseases [7]. This often implicates the evaluation of kinetic parameters of the
47 enzyme catalyzed reaction, such as: the maximal velocity (V_{\max}), the Michaelis-Menten constant
48 (K_m) or the turnover number (K_{cat}).

49 Additionally, the activity of an enzyme can be measured in the presence of modulatory molecules
50 that diminishes or enhances the enzyme's activity. This allows the evaluation of the degree of
51 modulation upon comparison to the innate enzymatic reaction, *i.e.* in the absence of modulatory
52 molecules. The half maximal inhibitory (IC_{50}) or activation (AC_{50}) concentrations are two
53 parameters that can be used to rank activators and inhibitors in terms of their potency in modulating
54 an enzyme's activity.

55 Another approach is to evaluate the equilibrium dissociation constant (K_d), or sometimes referred
56 to as K_i . K_d allows the prediction of the binding affinities between potential substrates/ligands and
57 target enzymes and is an important preliminary step for drug screening [8]. Both of these
58 approaches facilitate, through their complementarity, the establishment of a structure - activity
59 relationship (SAR) which can then act as a guideline for prioritizing certain ligands over others for
60 their therapeutic use [9].

61 All of the aforementioned parameters of enzymatic activity, modulation and binding affinities and
62 details will be revisited later on throughout this review. More details behind their conception and
63 applications can be acquired from several previous sources [10–13].

64 In addition to being drug targets themselves, enzymes can be used in the pharmaceutical industry
65 for the synthesis of active pharmaceutical compounds. Additionally, other industries such as the
66 food, biofuels and chemical industries have adapted the use of enzymes in their line of production
67 [14]. Some of the common examples for the implementation of enzymes in industrial processes
68 may be the production of lactose free dairy through the use of lactase enzymes [15] or in the
69 production of protease or lipase containing washing detergents [16].

70 For the last 10 years, various techniques have been reviewed and described for assaying enzymatic
71 activities as well as screening for drug candidates [6,9,17–25]. There exists no “one technique to

72 rule them all". Enzymes have different physical and chemical requirements and therefore some
73 assays may be unsuitable and must be modified or replaced. The choice of the technique depends
74 on several factors such as the relevance of the collected information, the price of the reagents and
75 the compatibility of the technique with the nature of the investigated enzymatic reaction [26].
76 Capillary electrophoresis (CE) is an analytical separative technique with applications in various
77 fields including enzymatic analysis. The substrate(s) and product(s) are separated in an open
78 capillary based on their charge-to-size ratio in an electric field applied across the capillary.
79 Enzymatic analysis with CE is associated with several advantages such as low sample and reagent
80 consumption, excellent separation efficiency and high versatility of hyphenation and operation
81 modes [27]. CE-based enzymatic reactions can be divided into pre-capillary (offline) and in-
82 capillary (online) reactions, where in the former, all the reagents, except one (substrate or enzyme),
83 are incubated in a vial outside the capillary [28]. The reaction is initiated by adding the missing
84 reagent (enzyme or substrate). Offline CE-assays are easy to optimize since the enzymatic reaction
85 and analyte separation occur independently. Due to this division in tasks, these assays are easy to
86 control. Manual interventions are, however, inevitable when handling reactions offline and
87 relatively large reaction volumes are required (few tens of μLs) [28,29]. On the other hand, with
88 the online CE reaction mode, the capillary acts as a nanoreactor in which the reaction, separation
89 and detection steps take place. There exist several methodologies by which the reactants are mixed
90 in-capillary such as electrophoretically mediated microanalysis (EMMA) [30,31] or transverse
91 diffusion of laminar flow profiles (TDLFP) [32]. These types of assays are often difficult to
92 optimize and to control due to the fact that all steps occur sequentially within the capillary.
93 Nonetheless, online assays are considerably more automated compared to offline ones.
94 CE can also be expanded to measure macromolecular binding interactions through the use of
95 affinity CE (ACE). This mode generally exploits the different electrophoretic mobilities of
96 unbound and bound complexes for their separation and quantification and may be fine-tuned
97 according to the application [33,34].
98 In terms of the overall performance, CE is often compared to the analytical technique widely used
99 by laboratories around the world, liquid chromatography (LC). Unlike CE, separation of analytes
100 in LC is based on their retention by a solid phase in a column. Although more commonly used for
101 separation of mixtures between two immiscible phases, LC have also been used for enzymatic
102 analysis [35].

103 Several recent papers have reviewed the state of the art of CE-based enzymatic analyses [36–38].
104 In this review, we go a step further by tracking the evolution, flexibility and adaptability of CE-
105 based enzymatic analyses through the use of two enzyme models, lipases and nucleoside kinases.
106 Both said enzymes have dissimilar modes of actions, reaction requirements and require different
107 analysis approaches making them thus suitable models of simple and complex reactions to
108 demonstrate the merits of CE-based enzymatic assays. Advantages and limitations of the CE-based
109 enzymatic assays will be highlighted and briefly compared to LC-based ones of the same caliber.
110 Furthermore, recently developed binding assays of lipases and kinases will be briefly discussed.

111

112 **2. CE-based lipase assays**

113 In this section, applications of CE utilizing lipases as model enzymes in drug screening, chiral
114 resolution, organic synthesis and enzyme characterization will be reviewed. A brief comparison
115 with LC-based approaches will be established when necessary in order to highlight on the
116 advantages and limitations of the analytical techniques. Furthermore, binding assays of lipases will
117 be briefly introduced.

118

119 ***2.1 General information about lipases***

120 Lipases (EC 3.1.1.3) belong to the hydrolases class of enzymes that catalyze the hydrolysis of ester
121 bonds such as those of triglycerides (TG) resulting in the release of free fatty acids (FFA) and
122 monoglyceride (MG), facilitating the absorption of fats into the body (Figure 1) [39]. Several
123 interesting applications have been described for lipases in different industrial fields such as in the
124 baking, dairy and pharmaceutical industry, production of cosmetics and detergents, synthesis of
125 bio-diesel or bioremediation processes [40–44]. Lipases-catalyzed reactions are rather
126 straightforward but operate with a unique mechanism of activation at the aqueous-fat/organic
127 interface (interfacial activation) [45,46]. Thanks to its versatility in operation modes and
128 hyphenation tactics, CE is a suitable technique for monitoring reactions catalyzed by lipases where
129 different types of products can be obtained.

130

131 ***2.2 Lipases activity and modulation***

132 Assessment of enzymatic activity can be helpful in identifying the presence or prove the absence
133 of an enzyme in a sample. Additionally, quantitative analyses of enzymatic reactions are crucial

134 for the understanding of the underlying mechanisms governing lipase reaction as well as the
135 subsequent biological and chemical consequences [47]. Enzymatic assays and the screening for
136 lipase inhibitors have been largely explored by CE [27,36,37,48–50] and HPLC [51–54].
137 The implication of CE in lipase-related studies was as early as the 1990s where it was used to
138 determine the purity of lipases from crude specimen [55,56]. In 1998, B. Vallejo-Cordoba *et al.*
139 introduced a CE assay to measure free fatty acids (FFA) in cream subjected to hydrolysis by lipases
140 [57]. FA with chain lengths of 4 – 12 carbons (C₄-C₁₂) were detected by adding p-anisate to the 20
141 mM tris BGE as a chromophore using indirect UV detection at $\lambda = 270$ nm. Methylated beta-
142 cyclodextrin (β -CD) was added to the BGE in order to enhance the solubility of FFA in the aqueous
143 solution through the formation of inclusion complexes, as previously described by L. Szente *et al.*
144 [58]. Conditions of the enzymatic reaction and CE separation are summarized in Table 1. The
145 kinetics of cream fat hydrolysis into FFA, catalyzed by a commercial lipase isolated from
146 *Rhizomucor miehei*, were followed by analyzing sample aliquots at different time periods for 60
147 min (Figure 2a).
148 The released FFA were analyzed using the CE method where a good separation of the individual
149 FFA species was obtained which allowed their quantification using pre-constructed calibration
150 curves. Figure 2b represents the electropherogram of resolved FFA species separated in only 10
151 min as anions of decreasing order of carbon chain length. Furthermore, it was revealed that short
152 chain FFA (C₄, C₆ and C₈) were the most abundant compared to larger ones at different reaction
153 times. The adopted CE method also permitted the detection and quantification of FFA in fresh
154 cream subjected to a MeOH extraction protocol. Compared to the FFA-extracted cream, higher
155 quantities of all FFA, especially those with short carbon chains, were detected in the lipolyzed one.
156 These short chain FFA play an important role in determining the flavor of dairy products [59,60].
157 The developed CE method overcame the requirements of FFA derivatization or extraction,
158 associated with chromatographic techniques such as gas chromatography (GC) and liquid
159 chromatography (LC). The study demonstrated the possibility of customizing dairy flavors by
160 blocking the lipase catalyzed hydrolysis of milk fat at specific times giving emphasis to short-
161 chains FFA production and providing an index for assessing milk quality.
162 Gang Hao *et al.* described an LC-quadruple time-of-flight (Q-TOF) MS method for assaying
163 microbial lipase activity [61]. The reaction mixture composed of lipase, triolein TG, 20% Triton-
164 X and incubation buffer (IB) was incubated at 37°C before injecting aliquots of 2 μ L collected at

165 different time points into LC-MS and measuring the amount of liberated oleic FA by using an
166 isotopically labeled [^{13}C]-oleic acid as an internal standard. LC was coupled to the Q-TOF MS by
167 an electrospray ionization (ESI) source. Mass spectra of oleic acid ($m/z = 281.25$) and the internal
168 standard ($m/z = 299.25$) were collected in the negative ionization mode at a capillary voltage of
169 2500 V. The method overcame the laborious radioactive or fluorescent labelling of the substrates
170 and the high pH requirements associated with conventional assays. A limitation of the described
171 assay compared to CE-based ones was the relatively high reagent concentrations which
172 necessitated a 500-fold dilution of the aliquoted reaction samples prior to their analysis.
173 Furthermore, the total injection volume of the samples collected sequentially over a period of 15
174 min ($5 \times 2 \mu\text{L}$) was one hundred-folds lower than the total volume of the reaction mixture (1 mL),
175 which meant that most of the sample was wasted especially since triolein hydrolyzed
176 spontaneously and had to be freshly prepared from stocks stored at freezing temperatures.

177 T. Koseki *et al.* [62] assayed the lipolytic activity of a recombinant lipase from filamentous fungi
178 *Aspergillus oryzae* (rLipAO), purified from an expression vector. Hydrolysis of tributyrin, a
179 natural TG found in butter, into butyrate was monitored using LC hyphenated to Q-TOF-MS and
180 CE hyphenated to TOF-MS. The lipolytic activity of rLipAO was compared to that of tannase, an
181 enzyme catalyzing the hydrolysis of ester and depside bonds, from the same fungal species. The
182 hydrolysis reaction was measured through the detection of lingering tributyrin after the reaction
183 by RP-LC-MS after injecting $1 \mu\text{L}$ of reaction mixture. CE-MS was used in the negative ionization
184 mode to monitor the release of butyric acid at m/z 87.045. Reaction and CE separation conditions
185 are summarized in Table 1. Figure 3 demonstrates the tributyrin hydrolysis reaction catalyzed by
186 rLipAO. The electropherogram represents the detection of butyrate peak at a migration time of
187 approximately 15 min in the presence of rLipAO. No butyrate peak was in the absence of rLipAO.
188 The isolated protein rLipAO demonstrated lipolytic activity toward the tributyrin substrate after 5
189 hr incubation at 37°C whilst *A. oryzae* tannase showed no activity.

190 This study demonstrated the practicality of CE-MS and its complementarity to LC-MS for the
191 characterization of the enzymatic activities of newly discovered proteins and protein fractions.
192 Moreover, enzyme immobilization offers them a higher tolerance to variations in temperatures and
193 pH and provides them with better storage stability [63,64]. It is argued that this increased tolerance
194 compared to in-solution enzymes is brought about by the lower flexibility of the amino acid

195 conformation of the immobilized enzymes, protecting them from thermal and pH-mediated
196 denaturation [63,65].

197 An online immobilized enzyme microreactor (IMER) was introduced by Y. Tang *et al.* in 2019
198 [66] to screen for lipase inhibitors. Pancreatic lipase (PL) was immobilized onto (3-
199 aminopropyl)triethoxysilane (APTES)-treated silica of the inner capillary walls *via* cross-linking
200 to a glutaraldehyde (GA) linker in three steps as illustrated in Figure 4a. The online enzymatic
201 hydrolysis of 4-nitrophenyl acetate (4-NPA) was then followed by measuring the peak area of the
202 4-NP product spectrophotometrically at $\lambda = 400$ nm. Following the optimization of acetonitrile
203 content in the enzymatic media, reaction pH and incubation time, the repeatabilities of the 4-NP
204 product peak area and migration time were evaluated. Using the same capillary provided good
205 peak areas and migration time repeatabilities (relative standard deviation or RSD < 5%) while the
206 RSD obtained using different capillaries were slightly higher but were still within the acceptable
207 range (< 15%) defined by international guidelines for validating analytical methodologies [67].
208 Immobilized lipase preserved 80% of its catalytic activity after 20 consecutive tests reflecting great
209 stability of the immobilized enzyme (Figure 4b, left). The affinity of immobilized PL towards 4-
210 NPA ($K_m = 2.7 \pm 0.29$ mM) was evaluated against a range of 4-NPA concentrations (0.6 - 7 mM)
211 (Figure 4b, right) and was almost two-folds greater compared to that of PL in solution ($K_m = 4.65$
212 ± 1.23 mM) This was attributed to a reduced steric hindrance between the immobilized PL
213 molecules and thus an increased contact between PL and the 4-NPA substrate. The IMER was used
214 to assay PL inhibition by orlistat, a reference PL inhibitor, as well as ten traditional Chinese
215 medicine extracts at 10 mg mL^{-1} by observing the decrease in 4-NP peak areas (Figure 4c).
216 Conditions of the enzymatic reaction and CE separation are summarized in Table 1. IC_{50} of orlistat
217 was evaluated as $0.0097 \mu\text{M}$, which was globally in good agreement with the literature. Six out of
218 the ten samples were demonstrated to possess mild to potent PL inhibition activity ranging from
219 21 to 70%. The developed method demonstrates the merits of enzyme immobilization, enhancing
220 both the affinity and activity of immobilized PL towards the 4-NPA substrate compared to in-
221 solution PL. Furthermore, the application of the method allowed rapid, automated and economic
222 analysis of PL inhibitors in complex plant extracts. The co-migration of some plant components
223 with the 4-NP product peak can be overcome by increasing the migratory distance to the detector.
224 Another lipase immobilization approach was introduced shortly after by Jai Liu *et al.* [68]. Using
225 the offline CE mode was used to search for inhibitors of immobilized *Candida rugose* lipase (CRL)

226 in traditional Tibetan medicines. CRL was attached onto titanium dioxide magnetic nanoparticles
227 ($\text{Fe}_3\text{O}_4@\text{TiO}_2$) which provides an efficient mean of low-cost enzyme immobilization as well as
228 the ability to separate the immobilized enzyme from the reaction medium due to the magnetic
229 nature of such NP. The group demonstrated several optimizations performed to enhance CRL
230 immobilization such as the pH, time and enzyme concentration. Furthermore, the activity of the
231 immobilized enzyme towards 4-nitrophenyl palmitate (4-NPP) was compared to that of in-solution
232 CRL. The release of 4-NP as a result of CRL-catalyzed hydrolysis of 4-NPP was monitored
233 spectrophotometrically at $\lambda = 400$ nm. Reaction and CE separation conditions are summarized in
234 Table 1. Compared to in-solution CRL, the immobilized enzyme was more active at high
235 temperatures (40 - 50°C) and preserved most of its 4-NPP hydrolyzing activity after storage at
236 4°C for 30 days whereas in-solution CRL lost around 65% of its activity. Furthermore,
237 immobilized CRL demonstrated higher affinity towards 4-NPP (2.51 mM) compared to CRL in
238 solution (9.96 mM). The inhibition kinetics of immobilized CRL were investigated against a range
239 of orlistat concentrations. A K_i value of 13.41 μM and an IC_{50} value of 4.37 mM was obtained for
240 orlistat. Moreover, amongst 6 methanolic extracts of traditional Chinese medicines, *Oxytropis*
241 *falcate* Bunge demonstrated considerable inhibition of immobilized CRL with 54 and 69%
242 inhibition at 50 and 100 mg mL^{-1} , respectively. Eleven compounds were identified and isolated
243 from *Oxytropis falcate* Bunge. They were screened individually for immobilized CRL inhibition
244 and compared to that of orlistat at 50 and 100 μM . Six out of the eleven compounds had promising
245 CRL inhibitory potentials similar to that of orlistat, which inhibited CRL by 64 and 82% at 50 and
246 100 μM , respectively. Kaempferol demonstrated superior inhibition to that of orlistat (92% at 50
247 and 100 μM). Kaempferol has been previously demonstrated as a CRL inhibitor and its inhibition
248 has been attributed to the high number of hydroxyl group in addition to their location on the
249 molecule [69]. In this study, lipase immobilization onto NP have shown to improve the enzyme's
250 durability, stability, reusability and, its affinity and activity towards the 4-NPP substrate compared
251 to in-solution lipases.

252 Y.-T. Zhu *et al.* introduced an HPLC-UV approach in 2014 to screen inhibition of porcine PL
253 immobilized covalently onto magnetic nanoparticles (NP) [70]. Several techniques such as atomic
254 force microscopy (AFM) and Fourier-transform infrared spectrometry (FT-IR) were used to
255 characterize the NP and the covalent binding of PL onto them.
256 Briefly, the amount of 4-NP liberated from the immobilized PL-catalyzed hydrolysis of 4-NPP,

257 was monitored at $\lambda = 317$ nm in the presence of reference PL inhibitors orlistat, (-)-
258 epigallocatechin 3-O-gallate (EGCG) and (-)-epigallocatechin (EGC) and compared to that in
259 their absence. The incubation of immobilized PL with the inhibitors was carried out offline prior
260 to injection. IC₅₀ values of 0.64 ± 0.02 μ M and 55 ± 0.5 μ M were calculated for orlistat and
261 EGCG, respectively, whereas no inhibitory effect was observed by EGC. As was the case in the
262 previous examples containing immobilized lipases, NP-PL demonstrated superior endurance to pH
263 and temperature changes as well as higher activity and affinity towards the 4-NPP substrate,
264 compared to in-solution lipases as suggested by higher V_{\max} (6.40 vs 3.16 U mg^{-1} enzyme) and
265 lower K_m (0.02 vs 0.29 mM) values, respectively. The total volume of the reaction mixture (4 mL)
266 used in this study by HPLC-UV were quite elevated and the retention time of the 4-NP product
267 was relatively long (≈ 19 min) whereas only 5 min were needed using CE-based assays of
268 immobilized lipases in the previous example.

269 Our group has recently developed and optimized the first homogeneous CE-based lipase assay
270 utilizing simultaneous double detection in the offline and online modes [71]. No immobilization
271 of PL or modifications of the capillary wall was needed. The reaction was monitored through the
272 detection of both products of the hydrolysis of 4-nitrophenyl butyrate (4-NPB) substrate, namely
273 4-NP by spectrophotometry ($\lambda = 400$ nm) and butyrate by capacitively coupled contactless
274 conductivity detector (C⁴D) (Figure 5a & b).

275 The capillary cartridge was supported by a home-made 3D-printed scaffold used to fasten both
276 UV and C⁴D detectors and ensure the circulation of the capillary cartridge coolant (Figure 5c).
277 Conditions of the online and offline CE-based assays are summarized in (Table 1). The Michaelis–
278 Menten constant (K_m) was evaluated as 0.57 ± 0.03 and 0.59 ± 0.12 mM ($n = 3$) using 4-NP and
279 butyrate, respectively. The maximum velocity (V_{\max}) was evaluated as 1.20 ± 0.13 and 0.71 ± 0.07
280 $\mu\text{M s}^{-1}$ ($n = 3$) using 4-NP and butyrate, respectively. Using the offline assay, extracts from three
281 plants, obtained *via* infusion in water, as well as a series of molecules isolated from oakwood and
282 wine extracts were all screened for PL modulation activities at 1 mg mL^{-1} ($n = 3$). Amongst the
283 plant extracts, those from fresh leaves of *Crataegus oxyacantha* (hawthorn) demonstrated the
284 strongest PL inhibition ($37 \pm 3\%$) whilst those from dry leaves of *Ribes nigrum* (black currant)
285 demonstrated the highest activation ($37 \pm 1.5\%$). Amongst the compounds isolated from oakwood
286 and wine extracts, two original triterpenoids were presented for the first time as potent PL
287 inhibitors, $51 \pm 1\%$ by bartogenic acid and $57 \pm 4\%$ by 3-O-galloylbarrinic acid. This inhibitory

288 effect was attributed to the presence of galloyl moieties or absence of glucosyl ones at specific
289 positions of the compounds. As far as we know, this is the only study that implicates CE-based PL
290 assays in a homogeneous phase with the other reactants.

291

292 **2.3 Enantioselective synthesis catalyzed by lipases**

293 CE has been established as a successful technique for chiral separations through the use of a chiral
294 selector in the BGE [72]. Lipases are known as chiral enzymes with stereo- and regioselective
295 properties favoring the formation of either enantiomers [73].

296 K. Pomeisl *et al.* [74] described an offline CE-based heterogeneous lipase assay using immobilized
297 lipase B from *Candida antarctica* (CALB) for the enantioselective resolution of *gem*-difluorinated
298 alcohols. These alcohols serve as intermediates in the synthesis of bioactive molecules with
299 potential anti-viral activities. The synthesis pathway of these fluorinated molecules is often
300 complicated. Additionally, the bioactivities of these molecules strongly depend on their
301 configuration. Lipase catalyzed enantioselective synthesis is thus an interesting approach for the
302 production of difluorinated bioactive molecules from alcohol derivatives. The group monitored
303 the progression of the transesterification reaction with time using CE/UV at $\lambda = 206$ nm. The
304 racemic (R and S) 3-(benzyloxy)-1-difluoropropanol alcohol substrates and subsequent racemic
305 ester products were detected and separated using sulfobutyl ether as a chiral selector in the
306 phosphoric acid (pH 2.5) BGE. The CE method allowed monitoring of enantiomeric substrate and
307 products in 14 min. The injection volume was very small (1-2 nL) making the method interesting
308 in analyzing reactions with low yields. The group identified a change of enantioselectivity when
309 changing the enzyme-to-substrate ratio from 1:1 to 5:1. They related these findings to the presence
310 of three reaction steps: acetylation, hydrolysis and isomerization.

311 A. Schuchert-Shi and P. C. Hauser [75] demonstrated the enantioselective hydrolysis of serine and
312 threonine amino acid esters by porcine PL using CE- C^4D . The use of conductimetry was essential
313 due to the inability to detect non-aromatic amino by UV spectrophotometry. The enantioselectivity
314 of the hydrolysis reaction was performed by temporal monitoring of the progression of the reaction
315 through the formation of the D- and L- amino acid, products. An acidic BGE, 2 M acetic acid,
316 containing 5 mM of the chiral selector (+)-(18-crown-6)-2,3,11,12-tetracarboxylic was used for
317 the chiral analyses. The separation of the DL-serine methyl esters (SME) substrate from the DL-
318 serine products and the enantiomeric resolution of D- and L- stereoisomers is demonstrated in

319 Figure 6.

320 The reaction was conducted by mixing PL with DL-SME or DL-threonine methyl esters (TME).
321 The group demonstrated the increased selectivity of PL towards the L-isoforms of both amino acid
322 methyl esters when assayed individually. Similarly, the enantioselectivity of PL was compared to
323 that of wheat germ lipase (WGL) using DL-SME hydrolysis. A consensus was established for the
324 favored production of L-serine by both PL and WGL with PL being more selective and having a
325 higher reaction rate. Between TME and SME, PL activity was higher towards the L-isoforms of
326 TME. This selectivity was related to a single structural difference manifested by a methyl group
327 unique to threonine and not to serine. Indeed, separation of molecules that differ only in their three-
328 dimensional configuration (stereoisomers) was possible with CE [76]. This was also demonstrated
329 in the studies utilizing lipases to catalyze enantioselective hydrolysis of chiral substrates.

330 Recently, Y. Choi *et al.* described an HPLC-based analytical method to determine the integral
331 stereoselectivity of lipases towards TG and DG [77]. This stereoselectivity considers the
332 preference of lipase hydrolysis towards all three ester bonds on the acylglycerol (TG and DG)
333 species. The detection required derivatization of the hydrolysis products with 4-nitrophenyl
334 isocyanate (4-NPI). In order to determine the integral stereoselectivity of porcine PL,
335 *Chromobacterium viscosum* lipase (CVL) and, *Pseudomonas fluorescens* lipase (PFL), the
336 enantiomeric excess of 1,2-DG over 1,3-DG was measured at different stages of the hydrolysis
337 reaction. Figure 7a represents the HPLC coupling to UV and evaporative light scattering detector
338 (ELSD). The 1,2- and 2,3-DG enantiomers were quantified using HPLC-UV at $\lambda = 285$ nm after
339 their derivatization. Using this method, it was shown that PL demonstrated no preference towards
340 ester bonds at positions (pos) 1 or 3 of the TG substrate, hydrolyzing them equally. Pos 2 ester
341 bonds were not hydrolyzed by PL. Moreover, a similar trend was observed for the hydrolysis of
342 DG into MG. For CVL, a contrast between the stereoselectivity towards ester bonds of TG and
343 DG was observed where the enzyme preferred pos 3 ester bonds over pos 1 in TG and the inverse
344 in DG. As was the case for PL, CVL did not hydrolyze ester bonds at pos 2. Finally, PFL
345 demonstrated hydrolysis of pos 2 ester bonds of TG. The stereoselectivity was thus in the order of
346 ester bonds at pos 1, 2 and 3 of TG. The method did not permit the determination of the exact
347 stereopreference of PFL towards DG isomers due to the presence of two possible hydrolysis sites
348 on each isomer. These results are represented in Figure 7b. The HPLC-based methods
349 demonstrated the ability to separate the different DG and MG isomers with good resolution and

350 separation factor (> 1). The isomers were then quantified using either HPLC-UV or HPLC-ELSD
351 which permitted the assessment of integral stereoselectivity of lipases from three biological
352 sources.

353 A drawback of the method was the need for isomer derivatization. Furthermore, although all three
354 DG isomers derivatives were detected in 13 min, the detection of MG isomers required the analyses
355 time to be extended to over 20 min. The reaction volume for HPLC-UV analyses (300 μ L) was
356 elevated compared to CE-based assays. A powerful green chromatographic technique to be used
357 for enantioresolution is supercritical fluid chromatography (SFC) where supercritical carbon
358 dioxide, possessing properties of both liquid and gas, is used as the mobile phase [78].

359 The previous examples demonstrate the efficiency of using CE for enantiomeric separation of
360 molecules, simply by adding a chiral selector in the BGE, and its power to separate products
361 obtained after enzymatic reaction in a relatively short time with minimal volume requirement.

362

363 **2.4 Organic synthesis**

364 The use of CE to monitor synthesis reactions is a promising prospect given the flexibility and the
365 low sample consumption of the technique. Furthermore, lipases have been used in biocatalyzed
366 organic synthesis reactions given their high catalytic activity, wide range of substrate specificity
367 and most importantly, their tolerance to high organic media [79].

368 W. Liu *et al.* [80] compared the activities of porcine PL immobilized onto different forms of porous
369 materials (metal-organic framework or MOF and SBA-15) by CE-UV through monitoring the
370 formation of anticoagulant-molecule, warfarin. The PL catalyzed synthesis reaction was carried
371 out by incubating PL with 4-hydroxycoumarin and benzylideneacetone, in methanol for 1 day at
372 50°C (Figure 8a). Reaction and CE conditions are summarized in Table 1. At the end of the
373 reaction, the solution was centrifuged for 5 min to separate the produced warfarin and residual
374 substrates into the supernatant and the carrier-PL complex into the residue.

375 This allowed the reusability of the immobilized PL. The supernatant was injected into the capillary
376 (0.5 psi x 3 sec; 3 nL) and a separation voltage of 28 kV was applied to separate the warfarin
377 product from the substrates using a borax buffer containing sodium dodecyl sulfate (SDS) as BGE
378 (pH 8.5). An example of the obtained electropherograms with PL immobilized onto MOF is
379 presented in Figure 8b. The warfarin yields by each of the PL immobilized onto 4 different MOFs
380 and SBA-15 in addition to in-solution PL were compared to assess catalytic activity and storage

381 of the immobilized enzyme. Compared to in-solution, all immobilized PL had higher activities
382 reflected by higher warfarin yields that did not change dramatically upon reusing after 5 cycles.
383 PL-MOFs had higher warfarin synthesizing activities compared to PL-SBA-15. The majority of
384 warfarin yield (65%) were maintained by PL-MOFs after storage for 35 days at 4°C. Additionally,
385 the RSD of warfarin yields using three batches of each PL-MOFs and their use across five cycles
386 was inferior to 3 % reflecting high catalytic stability. With 104 µL total reaction volume, 3 µL
387 injection volume and the ability to reuse the immobilized enzyme, the CE method for monitoring
388 warfarin synthesis was highly economic providing rapid separation of warfarin from the other
389 reactants in under 8 min.

390 The miniaturization of such organic reactions onto microchip systems with continuous flow
391 conjugated to appropriate detection techniques should be considered due to the advantages
392 provided at such scales especially the shorter reaction times [81].

393

394 **2.5 Binding assays of lipases**

395 In 2019, I. Hamdan *et al.* applied affinity CE to monitor changes in the migration times and peak
396 shapes of PL upon binding to certain drugs, orlistat or a combination of both [82]. CE was used to
397 confirm findings obtained using conventional spectrophotometric PL inhibition assays and
398 docking studies. Some of the tested drugs demonstrated synergism in inhibitory activity where the
399 addition of orlistat enhanced the overall inhibition. This was attributed to the binding mode of
400 these drugs to PL where the active site, *i.e.* orlistat binding site, remained exposed. Other drugs
401 demonstrated antagonism when combined with orlistat where the overall inhibition diminished
402 due to interferences with orlistat binding to the active site of PL. Orlistat, the tested drugs or both
403 were added to the 50 mM phosphate buffer (pH 6.8) containing 15% (v/v) ACN and 16.7% (v/v)
404 MeOH as BGE which was then used to fill the capillary. PL was then injected into the capillary.
405 As shown in Figure 9, PL (0.1 g L⁻¹) injected electrokinetically (18 kV × 15 s) into a capillary
406 filled with blank BGE (no ligands) was detected at 5.6 min by UV at $\lambda = 205$ nm. Once orlistat
407 alone was added to the BGE, a shift of PL migration time from 5.6 to 6.5 min was observed. This
408 was attributed to the binding of orlistat to PL favoring the migration of the complex towards the
409 anode, opposite to the direction of the EOF, and thus slowing down its migration in the capillary
410 by almost 1 min. Similarly, the presence of the tested drugs in the BGE resulted in a similar change
411 to PL in the capillary. When orlistat was present in combination with the drugs in the BGE, the

412 migration times shifts and peak shape changes were more drastic compared to the drugs or orlistat
413 alone (Figure 9a). One sole drug, dinitrosalicylic acid (DnS), did not demonstrate any significant
414 changes to the electropherograms upon addition of orlistat. This observation agreed with the results
415 obtained using PL inhibition assays and molecular docking studies (Figure 9b). DnS was shown
416 to bind strongly to Ser-152 of PL's active site which happens to be orlistat's binding site. Thus,
417 the overall inhibitory potential was reduced.

418 An interesting biophysical technique on the rise and used to evaluate biomolecular binding
419 affinities is microscale thermophoresis (MST) [83]. MST is based on the differential
420 thermodiffusion of bound and unbound species which is governed by the size, charge and solvation
421 of the analytes [83–85]. The technique is non-separative allowing the determination of K_d with
422 high sensitivity (in pM) in under 30 min and consuming miniscule amounts of samples ($\approx 4 \mu\text{L}$ for
423 each ligand concentration tested). Furthermore, using MST provides the analyst with the freedom
424 of choice of the buffer where practically any convenient solution or complex biological fluids can
425 be used. It has been previously applied for the evaluation of interactions between *E. Coli* AK and
426 ligands [86] as well as nucleoside diphosphate kinase (NDPK) and nucleoside analogs [87].
427 Additionally, our group used MST to evaluate the binding affinity between human neutrophil
428 elastase (HNE) and ursolic acid, a reference inhibitor of HNE ($K_d = 2.72 \pm 0.66 \mu\text{M}$) [88].

429 Recently, our group developed for the first time an MST-based binding assay to evaluate the
430 binding affinities of small ligands towards lipases from crude pancreatic extracts [89]. The
431 investigated ligands were purified from oakwood extracts and have been previously shown to
432 affect the activity of lipases either activating or inhibiting it using a CE-based assay [71]. The MST
433 protocol was optimized at different levels including the labeling protocol, storage and analysis
434 temperature and target concentrations. Once optimized, the MST method was used to titrate a fixed
435 concentration of the labeled lipases against a range of ligand concentrations. The K_d values were
436 evaluated for bartogenic acid (BA; $K_d = 1327 \pm 700 \text{ nM}$), 3-O-galloylbarrinic acid (3-GBA; $K_d =$
437 $500 \pm 300 \text{ nM}$) and Quercotriterpenoside-I (QTT-1; $K_d = 31 \pm 21 \text{ nM}$). The augmented standard
438 errors reflect poor repeatabilities of K_d evaluation possibly resulting from the fact that several types
439 of lipases are present simultaneously in the crude extracts. Enhancing the purity of the 50 kDa PL,
440 present in the extracts, by ammonium sulfate precipitation was successful although not compatible
441 with the MST labeling protocol. The obtained information is strictly restricted to the binding and
442 do not reflect the type of modulation this binding introduces to the lipase's activity. This became

443 problematic when the standard lipase inhibitor, orlistat, was considered. Due to the fact that orlistat
444 induces inhibition through covalent binding to the lipases active site and that MST are not suitable
445 to evaluate such type of irreversible binding interaction, using results from MST alone would give
446 the impression that orlistat and lipases do not interact.

447 The complementary use of activity-based assays by CE and binding affinity-based assays by MST
448 thus provides a better understanding of the molecular mechanism and paints a clearer image of the
449 modulation of catalytic activity resulting from ligand bindings.

450 The developed assay was successful in indicating a binding interaction between lipases and small
451 oakwood ligands despite using lipases from crude extracts which is a complex source of these
452 enzymes.

453

454 **3. CE-based nucleoside kinase assays**

455 This section will review some of the CE-based assays of nucleoside kinases. Unlike lipases,
456 applications of nucleoside kinases are mainly exclusive to scientific and pharmaceutical research.
457 Similar to the previous section, a brief comparison with LC-based approaches will be established
458 and nucleoside kinase binding assays will be briefly introduced.

459

460 **3.1 General information about nucleoside kinases**

461 Kinases (EC 2.7.x.x) belong to the family of phosphotransferases catalyzing the transfer of an
462 energetic phosphate group from a donor such as nucleotide triphosphates (NTP) toward an
463 acceptor. Kinases are divided into classes based on the type of phosphate group acceptors (*e.g.*:
464 proteins or nucleosides). Nucleoside kinases (EC 2.7.4.x) are essential for the phosphorylation of
465 nucleosides and nucleoside phosphates (nucleotides) playing major roles in processes such as the
466 nucleoside salvage pathways and DNA replication [90]. Figure 10 depicts the phosphorylation of
467 a nucleoside, thymidine, by thymidine kinase (TK), producing thymidine monophosphate (TMP)
468 and ADP. The phosphorylation of TMP to thymidine triphosphate (TTP) is then catalyzed by other
469 types of cellular nucleoside kinases. As is the case with other types of kinases, this reaction requires
470 the presence of a divalent metal cation to neutralize the negative charges of the phosphate groups
471 [90]. In this section, applications of CE for studies involving nucleoside kinases as models of more
472 complex enzymatic reactions with applications in scientific and pharmaceutical research will be
473 presented. Furthermore, kinases in general are often expensive to purchase and their production

474 require tedious work and may be time consuming. Therefore, it of interest to the manipulator to
475 use a technique such as CE that requires lower volumes of the enzymes in order to economize their
476 consumption.

477

478 **3.2 Nucleoside kinases activity and modulation**

479 In 1996, S. Banditelli *et al.* described a CE-based assay to monitor the activity of cytosolic 5'-
480 nucleotidase. Although not a kinase, cytosolic 5'-nucleotidase is a bifunctional enzyme
481 demonstrating phosphotransferase in addition to hydrolase activities [91]. Through the use of a
482 single CE-UV assay, both activities of 5'-nucleosidases were simultaneously monitored. The
483 method, summarized in Table 2, demonstrated an efficient separation of a mixture consisting of
484 several bases, nucleosides and nucleoside mono, di and triphosphates. The overall activity
485 (phosphatase + kinase) of the enzyme increased in the presence of a nucleoside phosphate acceptor
486 as demonstrated by the higher conversion of dGMP to dG in the presence of a nucleoside acceptor
487 such as inosine. Moreover, phosphorylation of deoxycytosine, an analog of adenosine used as
488 a chemotherapeutic drug, by the 5'-nucleotidase was demonstrated for the first time. This CE-UV
489 method was simple, rapid and required no labeling or modification of the substrates. Additionally,
490 the detection and efficient separation of the substrates and the products of both reactions catalyzed
491 by 5'-nucleotidase allowed the determination of the reaction rates corresponding to each activity
492 in a relatively short time (12 min) without the need of large sample quantities (10 nL).

493 H.-F. Tzeng *et al.* developed a CE-UV assay for measuring the activities of thymidine kinase (TK)
494 and thymidine monophosphate kinase (TMPK), simultaneously [92]. The method was optimized
495 for the detection of TMP and thymidine diphosphate (TDP), the products of thymidine
496 phosphorylation by TK and TMP phosphorylation by TMPK, respectively. A fused-silica bubble
497 cell capillary with an extended light path length of 150 μm to improve detection sensitivity [93].
498 Ethylenediaminetetraacetic acid (EDTA) was added in order to chelate Mg^{2+} co-factor ions which
499 were censured for the considerable ATP peak fronting due to the formation of ATP-Mg^{2+}
500 complexes. This resolved the ATP and TDP peaks which migrated close to one another. Mixing
501 the analyzed sample with NaCl and 66.7% ACN (*v/v*) prior to CE injection brought about several
502 improvements to the CE separation efficiency, peak shapes and mediated a sample stacking effect.
503 Indeed, slightly lower currents were achieved with ACN in addition to a 73% increase in the
504 apparent mobility difference between TDP and ATP species, enhancing the resolution of their

505 peaks by more than 100%. A 3-fold increase in the theoretical plate counts was achieved upon
506 addition of 20 mM NaCl to the sample treated with ACN. The optimized method was applied to
507 simultaneously detect TK and TMPK activities of the white spot syndrome virus (WSSV)-infected
508 insect cell line. Conditions of the enzymatic reaction as well as CE separation are summarized in
509 Table 2. After 10 min incubation of the cell protein extract with the reaction buffer at 37°C, TMP
510 and, to a lesser extent, TDP were detected confirming the presence of both TK and TMPK activities
511 (Figure 11). An additional 10 min incubation period at 37°C was sufficient to obtain a 170%
512 increase of TDP production, verifying the presence of TMPK activity in WSSV-infected cells. The
513 CE method provided a highly repeatable, rapid (6 min) and efficient separation of different
514 nucleosides in lysated cells. C. C. Liu *et al.*[94] described a CE-ESI-MS assay to monitor the
515 phosphorylation of lamivudine, an anti-retroviral drug, in human cell lines. Here, the negative
516 ionization mode was used as it provided similar detection sensitivities of both unphosphorylated
517 and phosphorylated nucleosides. The CE-MS method involved the use of a volatile ammonium
518 acetate solution as BGE. This allowed the separation of GMP from dGMP standards, differing
519 only by the presence of a hydroxyl group in GMP (Figure 12a). The developed method was then
520 applied to monitor the production of phosphorylated lamivudine metabolites in human cell line
521 extracts. Lamivudine is a cytosine analogue that is phosphorylated sequentially by cellular kinases
522 into active lamivudine triphosphate. The latter competes for incorporation into the RNA by reverse
523 transcriptases of viruses such as the human immunodeficiency virus (HIV) or hepatitis B virus
524 (HBV), blocking their replication. Conditions of the enzymatic reaction and CE-MS analysis are
525 summarized in Table 2. All three phosphorylated metabolites of lamivudine as well as lamivudine
526 itself were detected and separated in under 15 min verifying its activation in the human cell lines
527 (Figure 12b). In both previous examples, the developed CE-based nucleoside kinase assays were
528 validated through their application to living cells. The higher degree of complexity that cells
529 provide relative to *in-vitro* enzymatic assays attests to the credibility of the developed assays and
530 the interest of using CE for such analyses.

531 In 2006, J. Iqbal *et al.* described the development of three CE-based methods (Table 2) to assay
532 the activity and inhibition of adenosine kinase (AK) [95]. In the first method (Method A), the
533 micellar electrokinetic chromatography (MEKC) mode of CE-UV analysis was implemented
534 through the use of a BGE containing SDS. The MEKC-based method was used to test seven
535 adenosine nucleoside analogs, differing in the nature of substitution at position 2, as alternative

536 substrates of adenosine (Figure 13a). Only pyrrolidinyl- and isopropylamino-substituted analogues
537 showed relevant phosphorylation by AK, 53 and 81% respectively, compared to that of natural
538 AK substrate, adenosine. The combination of alkaline pH and high SDS content of the BGE (Table
539 2) ensured the separation of the analogue substrates of AK-catalyzed phosphorylation reactions
540 and their phosphorylated products. The second method (Method B) was quite similar to the first
541 one except for the BGE and the internal standard used (Table 2). It was applied to assess the
542 inhibition of AK by three standard AK inhibitors. A-134974, an analog of adenosine, was
543 identified as the most potent inhibitor according to the K_i values obtained using the developed CE-
544 based bovine AK assay as well as radioactive assays for bovine and human AK (Figure 13b). The
545 inhibition was assessed by measuring the extent of diminishing of the AMP product peak, detected
546 at 7 min, relative to a control AK-catalyzed reaction without inhibitors. The migration time of the
547 AMP peak was reduced by 2 min by increasing the pH of the BGE from 7.5 to 8.5. This is mainly
548 due to the increase in the magnitude of EOF sweeping all analytes towards the detector. The second
549 method thus permitted, in only 5 min, the calculation of kinetic inhibition parameters used to rank
550 AK inhibitors for their effectiveness.

551 Both of the methods described so far (A and B) involved carrying out AK-catalyzed reactions
552 offline. In the third method (Method C), the AK assay was carried out using the online CE-mode.
553 The capillary was coated with polyacrylamide to neutralize the silica charges on its walls and thus
554 to limit the interaction between charged groups on proteins and the capillary wall, a phenomenon
555 that often results in poor repeatabilities of migration times [96]. Furthermore, the use of a non-
556 alkaline BGE was necessary, since at high pH values, the neutral coating is less stable. For on-line
557 assay, a plug of the IB was first injected followed by sequentially injecting the enzymatic reactants.
558 The injection sequence was terminated by the injection of an IB plug and finally BGE. The partial
559 filling of the capillary with the IB plugs at the beginning and the end of the injection sequence
560 aims to isolate the reaction components from the BGE which could interfere with the reaction due
561 to its different pH. The reactants were mixed *via* EMMA after which the AMP product was allowed
562 to accumulate. The K_i values of the inhibitors obtained by this online assay agreed with those
563 obtained by the offline assay as well as by conventional radioactive assays where A-134974 was
564 the most potent inhibitor (Figure 13b). The online AK inhibition assay (method C) allowed the
565 adaptation of an automated, more economic form of the inhibition assays.

566 A similar example of this adaptability of CE was introduced a year later by the same group where
567 they introduced an optimized CE-UV approach to assay TK activity of the herpes simplex virus
568 (HSV) [97]. The phosphorylated product (dTMP) was detected in less than 7 min followed directly
569 by the UMP standard. However, interactions between charged protein groups of TK and the silanol
570 groups of the uncoated capillary led to variations in migration times and a decrease of the
571 separation quality and efficiency (Figure 14a). Therefore, the authors adapted the method by
572 masking the charged silanol groups by a polyacrylamide coating (Figure 14b). Indeed, a drastic
573 reduction in the RSD of migration times of dTMP was observed with coated capillaries (16-fold
574 lower, $n = 12$, Figure 14a). Furthermore, since the use of a neutral capillary required the reduction
575 of the BGE's pH, the BGE's ionic strength was increased to achieve good peak resolution in short
576 time. The use of electrokinetic injection allowed sample pre-concentration of anionic species and
577 increased sensitivity by approximately 7-fold (Figure 14a). Concerning the inner diameter of the
578 capillary, a higher diameter prompts higher detection sensitivities. However, the sensitivities of 75
579 μm capillaries were worse as more buffer ions are being introduced into the capillary by
580 electrokinetic injection (Figure 14a). The final conditions of the enzymatic reaction and CE
581 separation are summarized in Table 2. The optimized CE method was applied to assess 3
582 nucleoside analogues, acyclovir (ACV), (E)-5-(2-bromovinyl)-2'-deoxyuridine (BVDU) and
583 ganciclovir (GCV), as substrates of HSV TK (Figure 14c). In this example, parameters enhancing
584 the sensitivity of nucleotide detection as well as the repeatability of migration times by CE-UV
585 were adapted through implementing different strategies. The CE-method was adequately applied
586 in estimating kinetic parameters of each substrate which were in good agreement to previously
587 published values. Additionally, it was possible to assay the nature of TK inhibition by ACV using
588 the same method in around 6 min.

589 Similarly, our group applied a CE-UV method to determine the catalytic efficiency of human
590 TMPK [98]. The catalytic efficiency is measured as the ratio of K_{cat} to K_{m} which reflects the
591 effectiveness of the enzyme towards a particular substrate [99]. The catalytic efficiency of TMPK
592 obtained *via* CE towards TMP was then compared to that obtained using either flow injection
593 analysis coupled to high resolution mass spectrometry or spectrophotometric assays. The
594 concentration of the BGE, ammonium acetate, was relatively high in order to limit interactions
595 between the solutes and the capillary wall and enhances the repeatabilities of migration times
596 [100]. The TMPK enzymatic reaction was carried out in the presence of low concentrations of

597 MgCl₂ and ATP (co-factors) similar to those of FIA-HRMS analyses, as a compromise between
598 reduced ion suppression and adequate TMPK activity. The IB was a more diluted version of the
599 BGE to mediate a stacking effect due to the differences in conductivities of the injected sample
600 plug and the surrounding BGE [100,101]. This in turn enhances the shapes of the peaks and the
601 sensitivity of detection. Reaction and CE separation conditions are summarized in Table 2. This
602 method demonstrated the feasibility of carrying out kinetic evaluation of kinases using simply CE-
603 UV. The catalytic efficiency of the TMPK determined by CE-UV was in the same order of
604 magnitude compared to that determined by FIA-HRMS and conventional spectrophotometric
605 assays as depicted in Figure 15.

606 Concerning LC-based nucleoside kinase assays, only few examples can be found. This may be due
607 to the complex nature of the nucleoside kinase reaction and its media where analytes differing
608 by a single phosphate group may be difficult to separate. Additionally, the fact that most LC-based
609 analyses require the use of organic solvents is a hindering factor in the face of the development of
610 an online LC-based enzymatic assay. N. Malartre *et al.* introduced an HPLC-UV assay for
611 monitoring the phosphorylation activity of several different mutant variants of HSV-TK against
612 endogenous deoxythymidine and ACV [102]. The detection of the phosphorylated products was
613 possible in under 5 min, linear up to 0.22 mM with high sensitivity (LOD \approx 0.12 μ M). Based on
614 the phosphorylation activity of the mutant TK towards both deoxythymidine and ACV relative to
615 that of the wild-type TK, the proteins were classified into different classes providing means to
616 better understand antiviral resistance developed by HSV towards ACV on a genotypic and
617 phenotypic level.

618 Recently, C. Machon *et al.* introduced the first LC-HRMS assay to study 10 metabolites of 5-
619 fluorouracil (5-FU), a chemotherapeutic drug used to treat several types of cancers [103]. The LC-
620 MS method was first optimized for the detection of the different metabolites. The retention times
621 of some of the 5-FU metabolites were either very close or similar. 5-FU sequential phosphorylation
622 in HCT116 cells, human colon cancer cells, was confirmed by the indirect detection of 5-FUTP
623 metabolites. The developed method was demonstrated to be highly sensitive (in pg), selective
624 (discriminating 5-FU metabolites from endogenous ones) and linear (over a range of 0.5 - 3 million
625 cells) for the detection of 5-FU metabolites. Although the method demonstrated a great selectivity
626 towards 5-FU metabolites, due to the detection of specific fragmentation patterns of fluorine-
627 containing metabolites, the separation efficiency was rather low. This is a common limitation of

628 porous graphitic carbon columns, used in this study, were upon usage, loss of resolution and
629 retention capability is observed [104].

630 The abundance of CE-based nucleoside kinase assay relative to LC-based assays is a testimony of
631 the better adequacy of the former. CE have better adaptability and flexibility to resolve possible
632 issues. Furthermore, the low volume requirements and the little to no need for organic solvents
633 promote CE as an excellent separative technique for enzymatic analysis.

634

635 **3.3 Binding assays of nucleoside kinases**

636 One of the few binding assays of nucleoside kinases was developed by J. V. Pagaduan *et al.* using
637 a microchip electrophoresis to detect and quantify TK-1 in an immunocomplex using an anti-TK-
638 1 antibody (Ab) [105]. The assay was coupled to laser-induced fluorescence for the detection of
639 fluorescein isothiocyanate (FITC)-coupled Ab. The most suitable channel length was 5 mm as it
640 was sufficient for the separation of the unbound Ab from the TK-1/Ab immunocomplex. The
641 miniaturized assay was able to detect low concentrations (80 nM) of the immunocomplex in only
642 20 s. This assay however, was not applicable in its current form for the detection of TK-1 in serum
643 samples since the physiological or pathological concentrations of the enzyme were far lower than
644 the assay's detection limits (in the order of pM). Sample pre-concentration is one approach that
645 would allow the application of the developed miniaturized ME assay for determination of TK-1 in
646 biological samples.

647

648 **4. Conclusion**

649 In this review, the flexibility and reliability of CE for monitoring the catalytic activity reactions
650 and screening for potential modulators were demonstrated through the use of lipases which
651 produces a variety of products with different physical and chemical properties, and nucleoside
652 kinases which are precious and scarce samples when available. In-solution as well as immobilized
653 enzymes were successfully assayed using both offline and online CE modes coupled to different
654 detection techniques such as UV spectrophotometry, LIF, C⁴D and MS. The highly efficient
655 separation of the reaction components offered by CE comes in handy especially when the
656 substrates and products of the reaction are indiscernible from each other by standard
657 spectrophotometric approaches. The use of a wide array of synthetic and natural substrates was
658 possible and the modulation assay involved the use of various samples that ranged in complexity

659 from crude plant extracts and cell lysates to isolated and purified molecules. A possible drawback
660 encountered in some of the examples is associated with the use of complex samples which may
661 lead to less reliable results especially when using online CE-based assays. Compared to
662 chromatographic-based assays of lipases and nucleoside kinases, CE-based assays were faster,
663 required lower reaction and injection volumes and needed no organic solvents. The use of affinity
664 assays with the CE-based activity assays, complementarily, allows a better understanding of the
665 molecular mechanism behind ligand binding to the enzyme and of the modulation of its activity.
666 All these advantages conveyed by CE should expand its use in different application fields of
667 pharmaceutical and scientific research.

668

669 **5. Declaration**

670 **Authors' contribution**

671 Both G. Al Hamoui Dit Banni and R. Nehmé contributed equally to this work.

672 **Conflicts of interests**

673 The authors declare that there is no conflict of interests.

674 **Acknowledgements**

675 The authors would like to thank the Région Centre Val de Loire (PhD fellowship of G. Al Hamoui
676 Dit Banni) and the Labex SynOrg (ANR-11- LABX-0029) for financial support.

677 6. References

- 678 [1] G. Kapoor, S. Saigal, A. Elongavan, Action and resistance mechanisms of antibiotics: A
679 guide for clinicians, *J Anaesthesiol Clin Pharmacol.* 33 (2017) 300–305.
680 https://doi.org/10.4103/joacp.JOACP_349_15.
- 681 [2] Z. Lou, Y. Sun, Z. Rao, Current progress in antiviral strategies, *Trends Pharmacol. Sci.* 35
682 (2014) 86–102.
683 <https://doi.org/10.1016/j.tips.2013.11.006>.
- 684 [3] A. Sreedhar, Y. Zhao, Dysregulated metabolic enzymes and metabolic reprogramming in
685 cancer cells (Review), *Biomed Rep.* 8 (2018) 3–10. <https://doi.org/10.3892/br.2017.1022>.
- 686 [4] R. Nehmé, H. Nehmé, T. Saurat, M.-L. de Tauzia, F. Buron, P. Lafite, P. Verrelle, E.
687 Chautard, P. Morin, S. Routier, H. Bénédetti, New in-capillary electrophoretic kinase assays
688 to evaluate inhibitors of the PI3k/Akt/mTOR signaling pathway, *Anal. Bioanal. Chem.* 406
689 (2014) 3743–3754.
690 <https://doi.org/10.1007/s00216-014-7790-z>.
- 691 [5] B. Bonamichi, E.B. Parente, R.B. dos Santos, R. Beltzhoover, J. Lee, J.E.N. Salles, The
692 challenge of obesity treatment: a review of approved drugs and new therapeutic targets, *J.*
693 *Obes. Eat. Disord.* 4 (2018) 1–10.
694 <https://doi.org/10.21767/2471-8203.100034>.
- 695 [6] S. Fayad, P. Morin, R. Nehmé, Use of chromatographic and electrophoretic tools for
696 assaying elastase, collagenase, hyaluronidase, and tyrosinase activity, *J. Chromatogr. A.*
697 1529 (2017) 1–28.
698 <https://doi.org/10.1016/j.chroma.2017.11.003>.
- 699 [7] J. Strelow, W. Dewe, P.W. Iversen, H.B. Brooks, J.A. Radding, J. McGee, J. Weidner,
700 Mechanism of action assays for enzymes., in: S. Markossian, G.S. Sittampalam, A.
701 Grossman, K. Brimacombe, M. Arkin, D. Auld, C.P. Austin, J. Baell, J.M.M. Caaveiro,
702 T.D.Y. Chung, N.P. Coussens, J.L. Dahlin, V. Devanaryan, T.L. Foley, M. Glicksman,
703 M.D. Hall, J. V Haas, S.R.J. Hoare, J. Inglese, P.W. Iversen, S.D. Kahl, S.C. Kales, S.
704 Kirshner, M. Lal-Nag, Z. Li, J. McGee, O. McManus, T. Riss, P. Saradjian, O.J.J. Trask,
705 J.R. Weidner, M.J. Wildey, M. Xia, X. Xu (Eds.), *Assay Guid. Man.*, Bethesda (MD), 2004.
- 706 [8] M. Zeilinger, F. Pichler, L. Nics, W. Wadsak, H. Spreitzer, M. Hacker, M. Mitterhauser,
707 New approaches for the reliable in vitro assessment of binding affinity based on high-
708 resolution real-time data acquisition of radioligand-receptor binding kinetics, *EJNMMI*
709 *Res.* 7 (2017) 13.
710 <https://doi.org/10.1186/s13550-016-0249-9>.
- 711 [9] P.J. Tonge, Quantifying the interactions between biomolecules: guidelines for assay design
712 and data analysis, *Infect. Dis.* 5 (2019) 796–808.
713 <https://doi.org/10.1021/acsinfecdis.9b00012>.
- 714 [10] A. Cornish-Bowden, *Fundamentals of enzyme kinetics*, Elsevier Science, Amsterdam,
715 ND, 2014.
716 <https://books.google.fr/books?id=c4GQBQAAQBAJ>.

- 717 [11] H. Bisswanger, 2: General aspects of enzyme analysis, in: *Pract. Enzymol.*, Wiley-
718 Blackwell, 2012.
719 <https://doi.org/10.1002/9783527659227>.
- 720 [12] G.A. Holdgate, T.D. Meek, R.L. Grimley, Mechanistic enzymology in drug discovery: a
721 fresh perspective, *Nat. Rev. Drug Discov.* 17 (2018) 115–132.
722 <https://doi.org/10.1038/nrd.2017.219>.
- 723 [13] G.W. Caldwell, Z. Yan, W. Lang, J.A. Masucci, The IC 50 concept revisited, *Curr. Top.*
724 *Med. Chem.* 12 (2012) 1282–1290.
725 <https://doi.org/10.2174/156802612800672844>.
- 726 [14] J. Chapman, A.E. Ismail, C.Z. Dinu, Industrial applications of enzymes : recent advances,
727 techniques, and outlooks, *Catalysts.* 8 (2018) 1–26.
728 <https://doi.org/10.3390/catal8060238>.
- 729 [15] P.J.T. Dekker, D. Koenders, M.J. Bruins, Lactose-free dairy products: market
730 developments, production, nutrition and health benefits, *Nutrients.* 11 (2019) 1–14.
731 <https://doi.org/10.3390/nu11030551>.
- 732 [16] F.N. Niyonzima, S. More, Preparative biochemistry and biotechnology detergent-
733 compatible proteases : Microbial production , properties , and stain removal analysis, *Prep.*
734 *Biochem. Biotechnol.* 45 (2014) 233–258. <https://doi.org/10.1080/10826068.2014.907183>.
- 735 [17] R. Nehmé, P. Morin, Advances in capillary electrophoresis for miniaturizing assays on
736 kinase enzymes for drug discovery, *Electrophoresis.* 36 (2015) 2768–2797.
737 <https://doi.org/10.1002/elps.201500239>.
- 738 [18] N.S. El-Safory, A.E. Fazary, C.K. Lee, Hyaluronidases, a group of glycosidases: Current
739 and future perspectives, *Carbohydr. Polym.* 81 (2010) 165–181.
740 <https://doi.org/10.1016/j.carbpol.2010.02.047>.
- 741 [19] M. Stoytcheva, G. Montero, R. Zlatev, J.Á. León, V. Gochev, Analytical methods for
742 lipases activity determination: A Review, *Curr. Anal. Chem.* 8 (2012) 400–407.
743 <https://doi.org/10.2174/157341112801264879>.
- 744 [20] C.A. Espinosa-Leal, S. Garcia-Lara, Current methods for the discovery of new active
745 ingredients from natural products for cosmeceutical applications, *Planta Med.* 85 (2019)
746 535–551.
747 <https://doi.org/10.1055/a-0857-6633>.
- 748 [21] J.F. Glickman, 1. Assay development for protein kinase enzymes, in: S. Markossian, G.
749 Sittampalam, A. Grossman, K. Brimacombe, M. Arkin, D. Auld, C. P. Austin, J. Baell,
750 J.M.M. Caaveiro, T. D.Y. Chung, N. P. Coussens, J. L. Dahlin, V. Devanaryan, T. L. Foley,
751 M. Glicksman, M. D. Hall, J. V. Haas, S. R.J. Hoare, J. Inglese, P. W. Iversen, S. D. Kahl,
752 S.C. Kales, S. Kirshner, M. Lal-Nag, Z. Li, J. McGee, O. McManus, T. Riss, P. Saradjian,
753 O.J.J. Trask, J. R. Weidner, M. Jo Wildey, M. Xia, X. Xu (Eds.), *Assay Guid. Man.*, Eli
754 Lilly & Company and the National Center for Advancing Translational Sciences, Bethesda
755 (MD), 2004: pp. 1–19. <http://www.ncbi.nlm.nih.gov/pubmed/22553863>.
- 756 [22] Y. Wang, H. Ma, Protein kinase profiling assays: A technology review, *Drug Discov. Today*

- 757 Technol. 18 (2015) 1–8.
758 <https://doi.org/10.1016/j.ddtec.2015.10.007>.
- 759 [23] S. Lanka, A. Pradesh, J. Naveena, L. Latha, A short review on various screening methods
760 to isolate potential lipase producers: Lipases-the present and future enzymes of
761 biotechindustry, *Int. J. Biol. Chem.* 9 (2015) 207–219.
762 <https://doi.org/10.3923/ijbc.2015>.
- 763 [24] C. Peña-García, M. Martínez-Martínez, D. Reyes-Duarte, M. Ferrer, High throughput
764 screening of esterases, lipases and phospholipases in mutant and metagenomic libraries: A
765 Review, *Comb. Chem. High Through. Scr.* 19 (2016) 605–615.
766 <https://doi.org/10.2174/1386207319666151>.
- 767 [25] F. Hasan, A.A. Shah, A. Hameed, Methods for detection and characterization of lipases: A
768 comprehensive review, *Biotechnol. Adv.* 27 (2009) 782–798.
769 <https://doi.org/10.1016/j.biotechadv.2009.06.001>.
- 770 [26] J.P. Hughes, S.S. Rees, S.B. Kalindjian, K.L. Philpott, Principles of early drug discovery,
771 *Br. J. Pharmacol.* 162 (2011) 1239–1249.
772 <https://doi.org/10.1111/j.1476-5381.2010.01127.x>.
- 773 [27] M. Cheng, Z. Chen, Recent advances in screening of enzymes inhibitors based on capillary
774 electrophoresis, (2018).
775 <https://doi.org/10.1016/j.jpha.2018.05.002>.
- 776 [28] N. Banke, K. Hansen, I. Diers, Detection of enzyme activity in fractions collected from free
777 solution capillary electrophoresis of complex samples, *J. Chromatogr. A.* 559 (1991) 325–
778 335.
779 [https://doi.org/10.1016/0021-9673\(91\)80082-R](https://doi.org/10.1016/0021-9673(91)80082-R).
- 780 [29] H. Nehmé, Etude des réactions enzymatiques par électrophorèse capillaire, Etude des
781 réactions enzymatiques par électrophorèse capillaire, PhD Thesis, Université d'Orléans,
782 2013.
- 783 [30] J. Bao, F.E. Regnier, Ultramicro enzyme assays in a capillary electrophoretic system, *J.*
784 *Chromatogr. A.* 608 (1992) 217–224 .
785 [https://doi.org/10.1016/0021-9673\(92\)87127-t](https://doi.org/10.1016/0021-9673(92)87127-t).
- 786 [31] B.J. Harmon, D.H. Patterson, F.E. Regnier, Mathematical treatment of electrophoretically
787 mediated microanalysis, *Anal. Chem.* 65 (1993) 2655–2662.
788 <https://doi.org/10.1021/ac00067a018>.
- 789 [32] V. Okhonin, X. Liu, S.N. Krylov, Transverse diffusion of laminar flow profiles to produce
790 capillary nanoreactors, *Anal. Chem.* 77 (2005) 5925–5929.
791 <https://doi.org/10.1021/ac0508806>.
- 792 [33] Y. Wang, D.I. Adeoye, E.O. Ogunkunle, I.A. Wei, R.T. Filla, M.G. Roper, Affinity
793 capillary electrophoresis: A critical review of the literature from 2018 to 2020, *Anal. Chem.*
794 93 (2021) 295–310.
795 <https://doi.org/10.1021/acs.analchem.0c04526>.
- 796 [34] S. El Deeb, H. Wätzig, D.A. El-Hady, Capillary electrophoresis to investigate

- 797 biopharmaceuticals and pharmaceutically-relevant binding properties, *Trends Anal. Chem.*
798 48 (2013) 112–131.
799 <https://doi.org/10.1016/j.trac.2013.04.005>.
- 800 [35] D.O. Lambeth, W.W. Muhonen, High-performance liquid chromatography-based assays of
801 enzyme activities., *J. Chromatogr. B Biomed. Appl.* 656 (1994) 143–157.
802 [https://doi.org/10.1016/0378-4347\(94\)00072-7](https://doi.org/10.1016/0378-4347(94)00072-7).
- 803 [36] W.-F. Wang, J.-L. Yang, Advances in screening enzyme inhibitors by capillary
804 electrophoresis, *Electrophoresis* 40 (2019) 2075–2083.
805 <https://doi.org/10.1002/elps.201900013>.
- 806 [37] S. Gattu, C.L. Crihfield, G. Lu, L. Bwanali, L.M. Veltri, L.A. Holland, Advances in enzyme
807 substrate analysis with capillary electrophoresis, *Methods* 146 (2018) 93–106.
808 <https://doi.org/10.1016/j.ymeth.2018.02.005>.
- 809 [38] G.K.E. Scriba, F. Belal, Advances in capillary electrophoresis-based enzyme assays,
810 *Chromatographia* 78 (2015) 947–970 .
811 <https://doi.org/10.1007/s10337-015-2912-0>.
- 812 [39] B. Lindshield, Lipid digestion in the small intestine, in: *Intermed. Nutr.*, New Prairie Press,
813 Manhattan, 2018: pp. 443–445.
814 <https://newprairiepress.org/ebooks/19>.
- 815 [40] B. Andualema, A. Gessesse, Microbial lipases and their industrial applications, *Biotechnol.*
816 11 (2012) 100–118.
817 <https://doi.org/10.3923/biotech.2012.100.118>.
- 818 [41] R. Sindhu, S. Shiburaj, A. Sabu, P. Fernandes, R. Singhal, G. Marina, I.C. Nair, K.
819 Jayachandran, J. Vidya, L.P. de S. Vandenberghe, I. Deniz, A. Madhavan, P. Binod, R.K.
820 Sukumaran, S.S. Kumar, M. Anusree, N. Nagavekar, M. Soumya, A. Jayakumar, E.K.
821 Radhakrishnan, S.G. Karp, M. Giovana, M.G.B. Pagnoncelli, G.V. de M. Pereira, C.R.
822 Soccol, S. Dogan, A. Pandey, Enzyme technology in food processing : recent developments
823 and future prospects, in: *Innov. Food Process. Technol. A Compr. Rev.*, Elsevier,
824 Amsterdam, ND, 2021: pp. 191–215 .
825 <https://doi.org/10.1016/B978-0-12-815781-7.00016-0>.
- 826 [42] N.B. Melani, E.B. Tambourgi, E. Silveira, Lipases : from production to applications, *Sep.*
827 *Purif. Rev.* 49 (2020) 143–158.
828 <https://doi.org/10.1080/15422119.2018.1564328>.
- 829 [43] N. Sarmah, D. Revathi, G. Sheelu, K.Y. Rani, S. Sridhar, V. Mehtab, C. Sumana, Recent
830 advances on sources and industrial applications of lipases, *Biotechnol.* 34 (2018) 5–28.
831 <https://doi.org/10.1002/btpr.2581>.
- 832 [44] A. Houde, A. Kademi, D. Leblanc, Lipases and their industrial applications: an overview,
833 *Appl. Biochem. Biotechnol.* 118 (2004) 155–170.
834 <https://doi.org/10.1385/abab:118:1-3:155>.
- 835 [45] F.I. Khan, D. Lan, R. Durrani, W. Huan, Z. Zhao, Y. Wang, The lid domain in lipases:
836 structural and functional determinant of enzymatic properties, *Front. Bioeng. Biotechnol.* 5

- 837 (2017) 1–1 3.
838 <https://doi.org/10.3389/fbioe.2017.00016>.
- 839 [46] T. Zisis, P.L. Freddolino, P. Turunen, M.C.F. Van Teeseling, A.E. Rowan, K.G. Blank,
840 Interfacial activation of *Candida antarctica* lipase B: combined evidence from experiment
841 and simulation, *Biochemistry*. 54 (2015) 5969–5979.
842 <https://doi.org/10.1021/acs.biochem.5b00586>.
- 843 [47] H. Bisswanger, Enzyme assays, *Perspect. Sci.* 1 (2014) 41–55.
844 <https://doi.org/10.1016/j.pisc.2014.02.005>.
- 845 [48] J. Schejbal, G. Zdeněk, Immobilized-enzyme reactors integrated with capillary
846 electrophoresis for pharmaceutical research, *J. Sep. Sci.* 41 (2018) 323–335.
847 <https://doi.org/10.1002/jssc.201700905>.
- 848 [49] S. Huang, P. Paul, P. Ramana, E. Adams, P. Augustijns, A. Van Schepdael, Advances in
849 capillary electrophoretically mediated microanalysis for on-line enzymatic and
850 derivatization reactions., *Electrophoresis*. 39 (2018) 97–110.
851 <https://doi.org/10.1002/elps.201700262>.
- 852 [50] C.M. Ouimet, C.I. D'amico, R.T. Kennedy, Advances in capillary electrophoresis and the
853 implications for drug discovery., *Expert Opin. Drug Discov.* 12 (2017) 213–224.
854 <https://doi.org/10.1080/17460441.2017.1268121>.
- 855 [51] S.-Y. Shi, Y.-P. Zhang, X.-Y. Jiang, X.-Q. Chen, K.-L. Huang, H.-H. Zhou, X.-Y. Jiang,
856 Coupling HPLC to on-line, post-column (bio)chemical assays for high-resolution screening
857 of bioactive compounds from complex mixtures, *TrAC Trends Anal. Chem.* 28 (2009) 865–
858 877.
859 <https://doi.org/https://doi.org/10.1016/j.trac.2009.03.009>.
- 860 [52] A. De Simone, M. Naldi, M. Bartolini, L. Davani, V. Andrisano, Immobilized enzyme
861 reactors: an overview of applications in drug discovery from 2008 to 2018,
862 *Chromatographia*. 82 (2019) 425–441.
863 <https://doi.org/10.1007/s10337-018-3663-5>.
- 864 [53] S.-M. Fang, H.-N. Wang, Z.-X. Zhao, W.-H. Wang, Immobilized enzyme reactors in HPLC
865 and its application in inhibitor screening: A review, *J. Pharm. Anal.* 2 (2012) 83–89.
866 <https://doi.org/https://doi.org/10.1016/j.jpha.2011.12.002>.
- 867 [54] C.J. Malherbe, D. De Beer, E. Joubert, Development of on-Line high performance liquid
868 chromatography (HPLC)-biochemical detection methods as tools in the identification of
869 bioactives, *Int. J. Mol. Sci.* 13 (2012) 3101–3133.
870 <https://doi.org/10.3390/ijms13033101>.
- 871 [55] J.S. Hill, R.C. Davis, D. Yang, J. Wen, J.S. Philo, P.H. Poon, M.L. Phillips, E.S. Kempner,
872 H. Wong, Human hepatic lipase subunit structure determination, *J. Biol. Chem.* 271 (1996)
873 22931–22936.
874 <https://doi.org/10.1074/jbc.271.37.22931>.
- 875 [56] U. Bornscheuer, O.W. Reif, R. Lausch, R. Freitag, T. Scheper, F.N. Kolisis, U. Menge,
876 Lipase of *Pseudomonas cepacia* for biotechnological purposes: purification, crystallization

- 877 and characterization, *Biochim. Biophys. Acta.* 1201 (1994) 55–60.
878 [https://doi.org/10.1016/0304-4165\(94\)90151-1](https://doi.org/10.1016/0304-4165(94)90151-1).
- 879 [57] B. Vallejo-Cordoba, M.A. Mazorra-Manzano, A.F. González-Córdova, Determination of
880 short-chain free fatty acids in lipolyzed milk fat by capillary electrophoresis., *J. Capill.*
881 *Electrophor.* 5 (1998) 111–114.
- 882 [58] L. Szente, J. Szejtli, J. Szemán, L. Kató, Fatty acid-cyclodextrin complexes: Properties and
883 applications, *J. Incl. Phenom. Macrocycl. Chem.* 16 (1993) 339–354.
884 <https://doi.org/10.1007/BF00708714>.
- 885 [59] G. Amores, M. Virto, Total and free fatty acids analysis in milk and dairy fat, *Separations.*
886 6 (2019) 1–22.
887 <https://doi.org/10.3390/separations6010014>.
- 888 [60] M. Lubary, G.W. Hofland, J.H. ter Horst, The potential of milk fat for the synthesis of
889 valuable derivatives, *Eur. Food Res. Technol.* 232 (2011) 1–8.
890 <https://doi.org/10.1007/s00217-010-1387-3>.
- 891 [61] G. Hao, L. Yang, I. Mazsaroff, M. Lin, Quantitative determination of lipase activity by
892 liquid chromatography-mass spectrometry, *J. Am. Soc. Mass. Spectr.* 18 (2007) 1579–1581.
893 <https://doi.org/10.1016/j.jasms.2007.05.019>.
- 894 [62] T. Koseki, S. Asai, N. Saito, M. Mori, Y. Sakaguchi, K. Ikeda, Y. Shiono, Characterization
895 of a novel lipolytic enzyme from *Aspergillus oryzae*, *Appl. Microbiol. Biotechnol.* 97
896 (2013) 5351–5357.
897 <https://doi.org/10.1007/s00253-012-4391-7>.
- 898 [63] X. Chen, S. Xue, Y. Lin, J. Luo, L. Kong, Immobilization of porcine pancreatic lipase onto
899 a metal-organic framework, PPL@MOF: A new platform for efficient ligand discovery
900 from natural herbs, *Anal. Chim. Acta.* 1099 (2020) 94–102.
901 <https://doi.org/10.1016/j.aca.2019.11.042>.
- 902 [64] J. Iqbal, S. Iqbal, C.E. Müller, Advances in immobilized enzyme microreactors in
903 capillary electrophoresis, *Analyst.* 138 (2013) 3104–3116.
904 <https://doi.org/10.1039/c3an00031a>.
- 905 [65] U. Guzik, K. Hupert-kocurek, D. Wojcieszynska, Immobilization as a strategy for
906 improving enzyme properties-Application to oxidoreductases, *Molecules.* 19 (2014) 8995–
907 9018.
908 <https://doi.org/10.3390/molecules19078995>.
- 909 [66] Y. Tang, W. Li, Y. Wang, Y. Zhang, Y. Ji, Rapid on-line system for preliminary screening
910 of lipase inhibitors from natural products by integrating capillary electrophoresis with
911 immobilized enzyme microreactor, *J. Sep. Sci.* 43 (2019) 1003–1010.
912 <https://doi.org/10.1002/jssc.201900523>.
- 913 [67] S. Kollipara, G. Bende, A.Á. Ema, Á. Regulatory, International guidelines for bioanalytical
914 method validation : A comparison and discussion on current scenario, *Chromatographia.* 73
915 (2011) 201–217.
916 <https://doi.org/10.1007/s10337-010-1869-2>.

- 917 [68] J. Liu, R.-T. Ma, Y.-P. Shi, An immobilization enzyme for screening lipase inhibitors from
918 Tibetan medicines, *J. Chromatogr. A.* 1615 (2020) 1–8.
919 <https://doi.org/10.1016/j.chroma.2019.460711>.
- 920 [69] C. Ruiz, S. Falcocchio, E. Xoxi, L. Villo, G. Nicolosi, F.I.J. Pastor, P. Diaz, L. Saso,
921 Inhibition of *Candida rugosa* lipase by saponins, flavonoids and alkaloids, *J. Mol. Catal. B*
922 *Enzym.* 40 (2006) 138–143.
923 <https://doi.org/10.1016/j.molcatb.2006.02.012>.
- 924 [70] Y. Zhu, X. Ren, Y. Liu, Y. Wei, L. Qing, X. Liao, Covalent immobilization of porcine
925 pancreatic lipase on carboxyl-activated magnetic nanoparticles: Characterization and
926 application for enzymatic inhibition assays, *Mater. Sci. Eng. C.* 38 (2014) 278–285.
927 <https://doi.org/10.1016/j.msec.2014.02.011>.
- 928 [71] G. Al Hamoui Dit Banni, R. Nasreddine, S. Fayad, P.C. Ngoc, J.C. Rossi, L. Leclercq, H.
929 Cottet, A. Marchal, R. Nehmé, Screening for pancreatic lipase natural modulators by
930 capillary electrophoresis hyphenated to spectrophotometric and conductometric dual
931 detection, *Analyst.* 146 (2021) 1386–1401.
932 <https://doi.org/10.1039/D0AN02234A>.
- 933 [72] S. Bernardo-Bermejo, E. Sánchez-López, M. Castro-Puyana, M.L. Marina, Chiral capillary
934 electrophoresis, *Trends Anal. Chem.* 124 (2020) 1–18.
935 <https://doi.org/10.1016/j.trac.2020.115807>.
- 936 [73] K.K. Bhardwaj, R. Gupta, Synthesis of chirally pure enantiomers by lipase, *J. Oleo Sci.* 66
937 (2017) 1073–1084.
938 <https://doi.org/10.5650/jos.ess17114>.
- 939 [74] K. Pomeisl, N. Lamatová, V. Šolínová, R. Pohl, J. Brabcová, V. Kašička, M. Krečmerová,
940 Enantioselective resolution of side-chain modified gem-difluorinated alcohols catalysed by
941 *Candida antarctica* lipase B and monitored by capillary electrophoresis, *Bioorganic Med.*
942 *Chem.* 27 (2019) 1246–1253.
943 <https://doi.org/10.1016/j.bmc.2019.02.022>.
- 944 [75] A. Schuchert-Shi, P. C. Hauser, Following the lipase catalyzed enantioselective hydrolysis
945 of amino acid esters with capillary electrophoresis using contactless conductivity detection,
946 *Chirality.* 22 (2010) 331–335.
947 <https://doi.org/10.1002/chir.20746>.
- 948 [76] B. Chankvetadze, W. Linder, G.K.E. Schriba, Enantiomer separations in capillary
949 electrophoresis in the case of equal binding constants of the enantiomers with a chiral
950 selector: Commentary on the feasibility of the concept, *Anal. Chem.* 76 (2004) 4256–4260.
951 <https://doi.org/10.1021/ac0355202>.
- 952 [77] Y. Choi, J.-Y. Park, P.-S. Chang, Integral stereoselectivity of lipase based on the
953 chromatographic resolution of enantiomeric/regioisomeric diacylglycerols, *J. Agric. Food*
954 *Chem.* 69 (2021) 325–331.
955 <https://doi.org/10.1021/acs.jafc.0c07430>.
- 956 [78] C. West, Recent trends in chiral supercritical fluid chromatography, *Trends Anal. Chem.*

- 957 120 (2019) 1–9.
958 <https://doi.org/10.1016/j.trac.2019.115648>.
- 959 [79] A. Kumar, K. Dhar, S.S. Kanwar, P.K. Arora, Lipase catalysis in organic solvents:
960 advantages and applications, *Biol. Proced. Online.* 18 (2016) 1–11.
961 <https://doi.org/10.1186/s12575-016-0033-2>.
- 962 [80] W.L. Liu, N.S. Yang, Y.T. Chen, S. Lirio, C.Y. Wu, C.H. Lin, H.Y. Huang, Lipase-
963 supported metal-organic framework bioreactor catalyzes warfarin synthesis, *Chem. Eur. J.*
964 21 (2015) 115–119.
965 <https://doi.org/10.1002/chem.201405252>.
- 966 [81] S.F.Y. Li, L.J. Kricka, Clinical analysis by microchip capillary electrophoresis, *Clin. Chem.*
967 52 (2006) 37–45.
968 <https://doi.org/10.1373/clinchem.2005.059600>.
- 969 [82] I. Hamdan I., H. Zalloum, Pancreatic lipase inhibitory activity of selected pharmaceutical
970 agents, *Acta Pharm.* 69 (2019) 1–16.
- 971 [83] C.J. Wienken, P. Baaske, U. Rothbauer, D. Braun, S. Duhr, Protein-binding assays in
972 biological liquids using microscale thermophoresis, *Nat. Commun.* 1 (2010) 1–7.
973 <https://doi.org/10.1038/ncomms1093>.
- 974 [84] M. Jerabek-Willemsen, C.J. Wienken, D. Braun, P. Baaske, S. Duhr, Molecular interaction
975 studies using microscale thermophoresis, *Assay Drug Dev. Technol.* 9 (2011) 342–353.
976 <https://doi.org/10.1089/adt.2011.0380>.
- 977 [85] M. Jerabek-Willemsen, T. André, R. Wanner, H.M. Roth, S. Duhr, P. Baaske, D.
978 Breitsprecher, Microscale thermophoresis: interaction analysis and beyond, *J. Mol. Struct.*
979 1077 (2014) 101–113.
980 <https://doi.org/10.1016/j.molstruc.2014.03.009>.
- 981 [86] H. Mazal, H. Aviram, I. Riven, G. Haran, Effect of ligand binding on a protein with a
982 complex folding landscape, *Phys. Chem. Chem. Phys.* 20 (2018) 3054–3062.
983 <https://doi.org/10.1039/c7cp03327c>.
- 984 [87] S. Priet, L. Roux, M. Saez-Ayala, F. Ferron, B. Canard, K. Alvarez, Enzymatic synthesis of
985 acyclic nucleoside thiophosphonate diphosphates: Effect of the α -phosphorus configuration
986 on HIV-1 RT activity, *Antivir. Res.* 117 (2015) 122–131.
987 <https://doi.org/10.1016/j.antiviral.2015.03.003>.
- 988 [88] F. Syntia, R. Nehmé, B. Claude, P. Morin, Human neutrophil elastase inhibition studied by
989 capillary electrophoresis with laser induced fluorescence detection and microscale
990 thermophoresis, *J. Chromatogr. A.* 1431 (2016) 215–223.
991 <https://doi.org/10.1016/j.chroma.2015.12.079>.
- 992 [89] G. Al Hamoui Dit Banni, R. Nasreddine, S. Fayad, C. Colas, A. Marchal, R. Nehmé,
993 Investigation of lipase-ligand interactions in porcine pancreatic extracts by microscale
994 thermophoresis, *Anal. Bioanal. Chem.* 413 (2021) 3667–3681.
995 <https://doi.org/10.1007/s00216-021-03314-7>.
- 996 [90] D. Deville-bonne, C. El, P. Meyer, Y. Chen, L.A. Agrofoglio, J. Janin, Human and viral

- 997 nucleoside/nucleotide kinases involved in antiviral drug activation: structural and catalytic
998 properties, *Antivir. Res.* 86 (2010) 101–120.
999 <https://doi.org/10.1016/j.antiviral.2010.02.001>.
- 1000 [91] S. Banditelli, C. Baiocchi-ii, R. Pesi, S. Allegrini, M. Turriani, P.L. Ipata, M.C.A.M. Ici,
1001 M.G. Tozzi, The phosphotransferase activity of cytosolic 5'-nucleotidase ; a purine analog
1002 phosphorylating enzyme, *Int. J. Biochem. Cell Biol.* 28 (1996) 711–720.
1003 [https://doi.org/https://doi.org/10.1016/1357-2725\(95\)00171-9](https://doi.org/https://doi.org/10.1016/1357-2725(95)00171-9).
- 1004 [92] H. Tzeng, H. Hung, Simultaneous determination of thymidylate and thymidine diphosphate
1005 by capillary electrophoresis as a rapid monitoring tool for thymidine kinase and thymidylate
1006 kinase activities, *Electrophoresis.* 26 (2005) 2225–2230.
1007 <https://doi.org/10.1002/elps.200410091>.
- 1008 [93] T. Drevinskas, L. Telksnys, A. Maruška, J. Gorbatsova, M. Kaljurand, Capillary
1009 electrophoresis sensitivity enhancement based on adaptive moving average method, *Anal.*
1010 *Chem.* 90 (2018) 6773–6780.
1011 <https://doi.org/10.1021/acs.analchem.8b00664>.
- 1012 [94] C.C. Liu, J.S. Huang, D.L.J. Tyrrell, N.J. Dovichi, Capillary electrophoresis-electrospray-
1013 mass spectrometry of nucleosides and nucleotides: Application to phosphorylation studies
1014 of anti-human immunodeficiency virus nucleosides in a human hepatoma cell line,
1015 *Electrophoresis.* 26 (2005) 1424–1431.
1016 <https://doi.org/10.1002/elps.200410423>.
- 1017 [95] J. Iqbal, B. Joachim C, M. Christa E, Development of off-line and on-line capillary
1018 electrophoresis methods for the screening and characterization of adenosine kinase
1019 inhibitors and substrates, *Electrophoresis.* 27 (2006) 2505–2517.
1020 <https://doi.org/10.1002/elps.200500944>.
- 1021 [96] R. Nehmé, C. Perrin, V. Guerlavais, J.A. Fehrentz, H. Cottet, J. Martinez, H. Fabre, Use of
1022 coated capillaries for the electrophoretic separation of stereoisomers of a growth hormone
1023 secretagogue, *Electrophoresis.* 30 (2009) 3772–3779.
1024 <https://doi.org/10.1002/elps.200900093>.
- 1025 [97] J. Iqbal, L. Scapozza, G. Folkers, E.M. Christa, Development and validation of a capillary
1026 electrophoresis method for the characterization of herpes simplex virus type 1 (HSV-1)
1027 thymidine kinase substrates and inhibitors, *J. Chromatogr. B.* 846 (2007) 281–290.
1028 <https://doi.org/10.1016/j.jchromb.2006.09.018>.
- 1029 [98] J. Ferey, D. Da Silva, C. Colas, R. Nehmé, P. Lafite, V. Roy, P. Morin, R. Daniellou, L.
1030 Agrofoglio, B. Maunit, Monitoring of successive phosphorylations of thymidine using free
1031 and immobilized human nucleoside / nucleotide kinases by Flow Injection Analysis with
1032 High-Resolution Mass Spectrometry, *Anal. Chim. Acta.* 1049 (2019) 115–122.
1033 <https://doi.org/10.1016/j.aca.2018.10.032>.
- 1034 [99] R. Roskoski, Michaelis-Menten kinetics, in: *Ref. Modul. Biomed. Sci.*, Elsevier, 2015.
1035 <https://doi.org/https://doi.org/10.1016/B978-0-12-801238-3.05143-6>.
- 1036 [100] H. Whately, Basic principles and modes of capillary electrophoresis, in: J. Petersen, A.A.

- 1037 Mohammad (Eds.), *Clin. Forensic Appl. Capill. Electrophor.*, Humana Press, New Jersey,
1038 2001: pp. 21–58.
1039 <https://doi.org/10.1007/978-1-59259-120-6>.
- 1040 [101] D.N. Heiger, *High performance capillary electrophoresis: an introduction: a primer*,
1041 Agilent Technologies, Germany, 2000. <https://books.google.fr/books?id=6KGJgEACAAJ>.
- 1042 [102] N. Malartre, R. Boulieu, N. Falah, J.C. Cortay, B. Lina, F. Morfin, E. Frobert, Effects of
1043 mutations on herpes simplex virus 1 thymidine kinase functionality: an in vitro assay based
1044 on detection of monophosphate forms of acyclovir and thymidine using HPLC/DAD,
1045 *Antivir. Res.* 95 (2012) 224–228. <https://doi.org/10.1016/j.antiviral.2012.07.001>.
- 1046 [103] C. Machon, F. Catez, N.D. Venezia, F. Vanhalle, L. Guyot, A. Vincent, M. Garcia, B. Roy,
1047 J.J. Diaz, J. Guitton, Intracellular anabolism of 5-fluorouracil and incorporation in nucleic
1048 acids based on an LC-HRMS method, *J. Pharm. Anal.* 11 (2021) 77–87.
1049 <https://doi.org/https://doi.org/10.1016/j.jpha.2020.04.001>.
- 1050 [104] S. Bustamante, R.B. Gilchrist, D. Richani, A sensitive method for the separation and
1051 quantification of low-level adenine nucleotides using porous graphitic carbon-based liquid
1052 chromatography and tandem mass spectrometry, *J. Chromatogr. B.* 1061–1062 (2017) 445–
1053 451.
1054 <https://doi.org/10.1016/j.jchromb.2017.07.044>.
- 1055 [105] J. V Pagaduan, M. Ramsden, K.O. Neill, A.T. Woolley, Microchip immunoaffinity
1056 electrophoresis of antibody – thymidine kinase 1 complex, *Electrophoresis.* 36 (2015) 813–
1057 817.
1058 <https://doi.org/10.1002/elps.201400436>.
- 1059

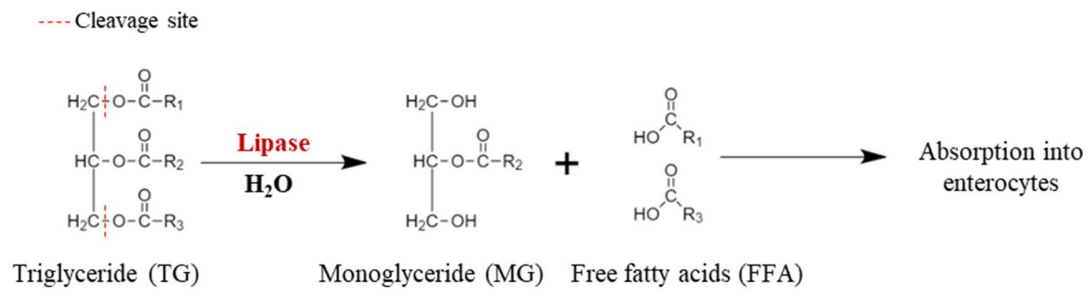


Figure 1: An illustration of TG hydrolysis catalyzed by lipases

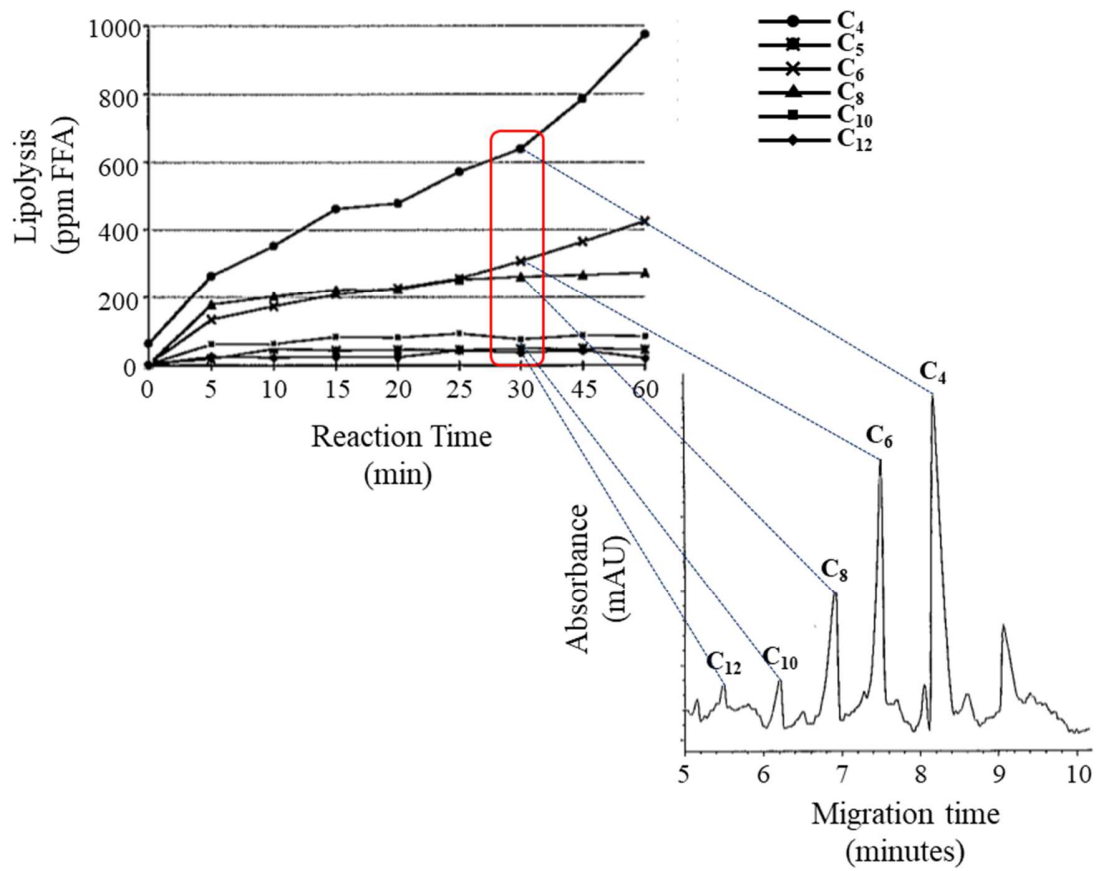


Figure 2: Kinetics of lipase catalyzed hydrolysis of cream fat into FFA (a) and, electropherogram of FFA in lyophilized cream for 30 min (b). Adapted from [57]. Reaction and separation conditions are summarized in Table 1

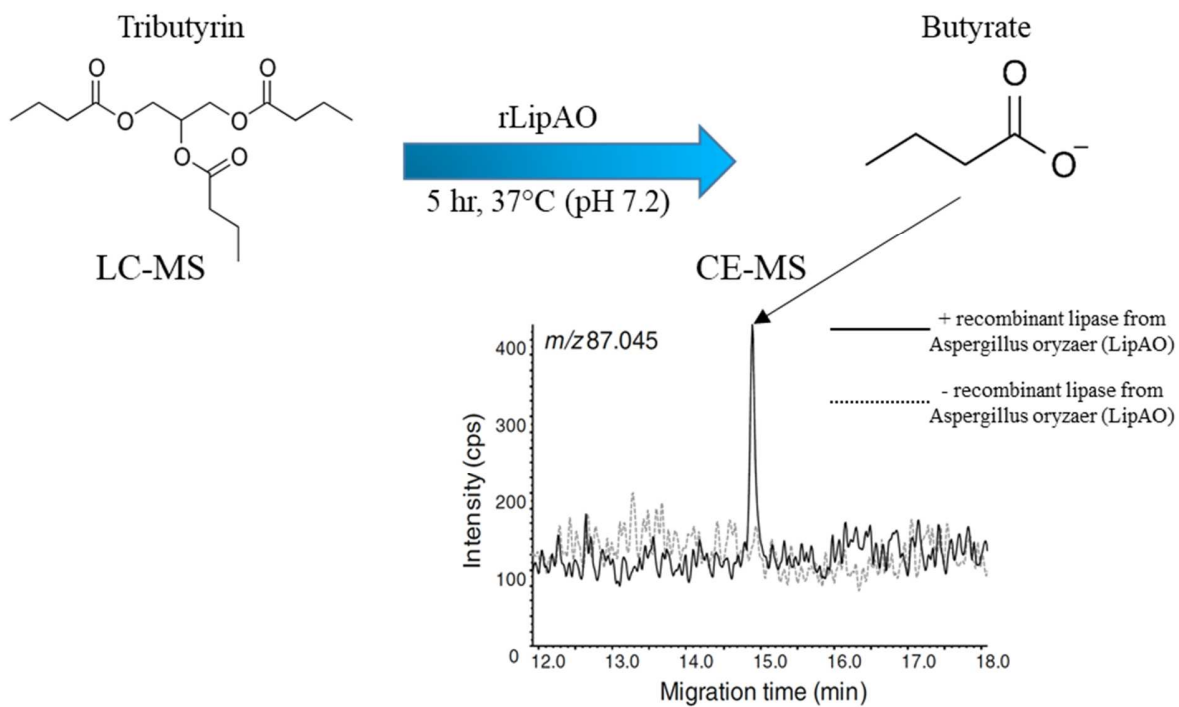
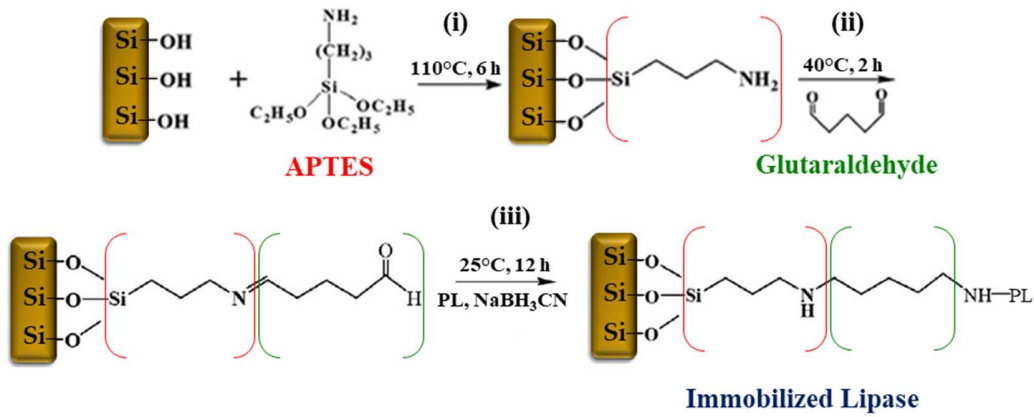
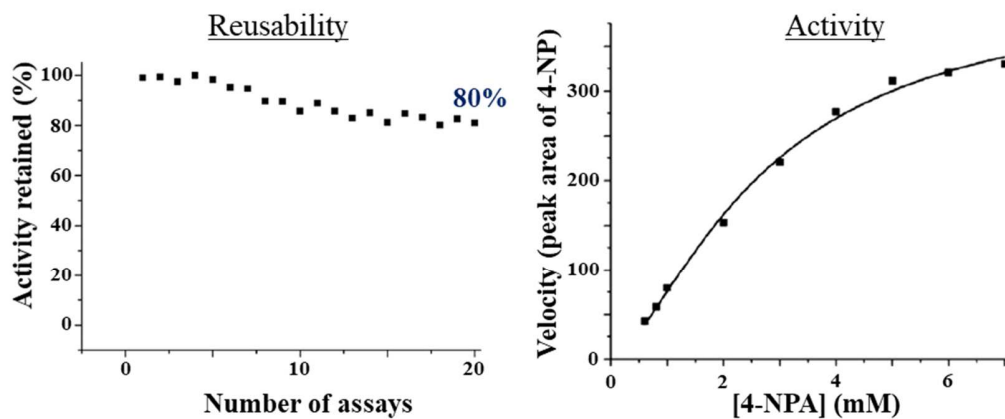


Figure 3: Hydrolysis of tributyrin by rLipAO from *Aspergillus oryzae* into butyrate detected by CE-TOF-MS as depicted in the electropherogram. The tributyrin substrate was monitored using LC-(Q-TOF-MS). Conditions of the enzymatic reaction, LC-MS and CE-MS are summarized in Table 1. Adapted from [62]

(a) PL immobilization *via* cross-linking



(b) Characterization of immobilized PL



(c) Inhibitor screening

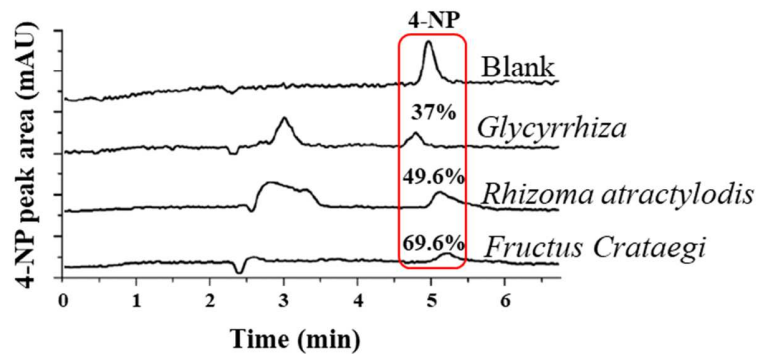


Figure 4: Illustration of PL immobilization onto the capillary wall *via* cross-linking using glutaraldehyde as a bifunctional linker (a), Immobilized PL reusability over 20 assays and activity over a range of 4-NPB concentrations (0.6-7 mM) (b) and, Screening of plant extracts at 10 mg mL^{-1} for PL inhibition (c). More conditions of enzymatic reaction, inhibition assays and CE separation are summarized in Table 1. Adapted from [66]

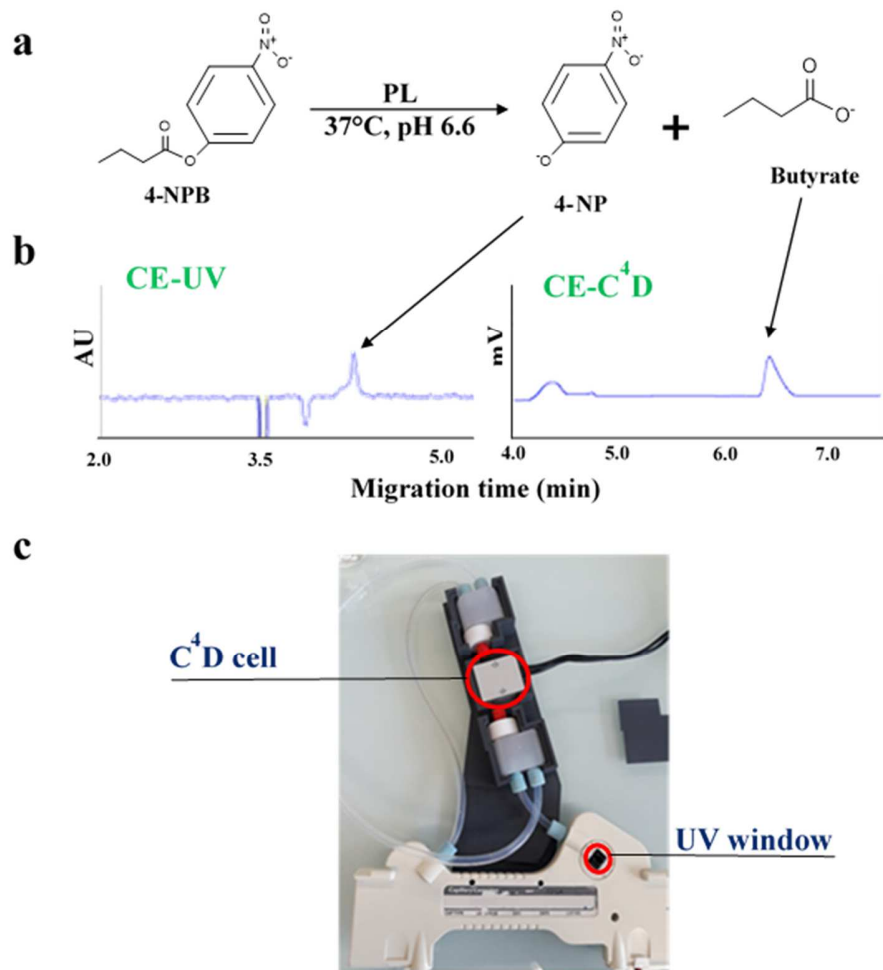


Figure 5: Lipase-catalyzed hydrolysis of 4-NPB into 4-NP and butyrate (a). Electropherograms for the detection of 4-NP and butyrate individually by CE-UV and CE-C⁴D, respectively (b). Demonstration of the dual detector cartridge with an adapted 3D-printed scaffold (c). Adapted from [71]

(1)-(18-crown-6)-2,3,11,12-tetracarboxylic acid

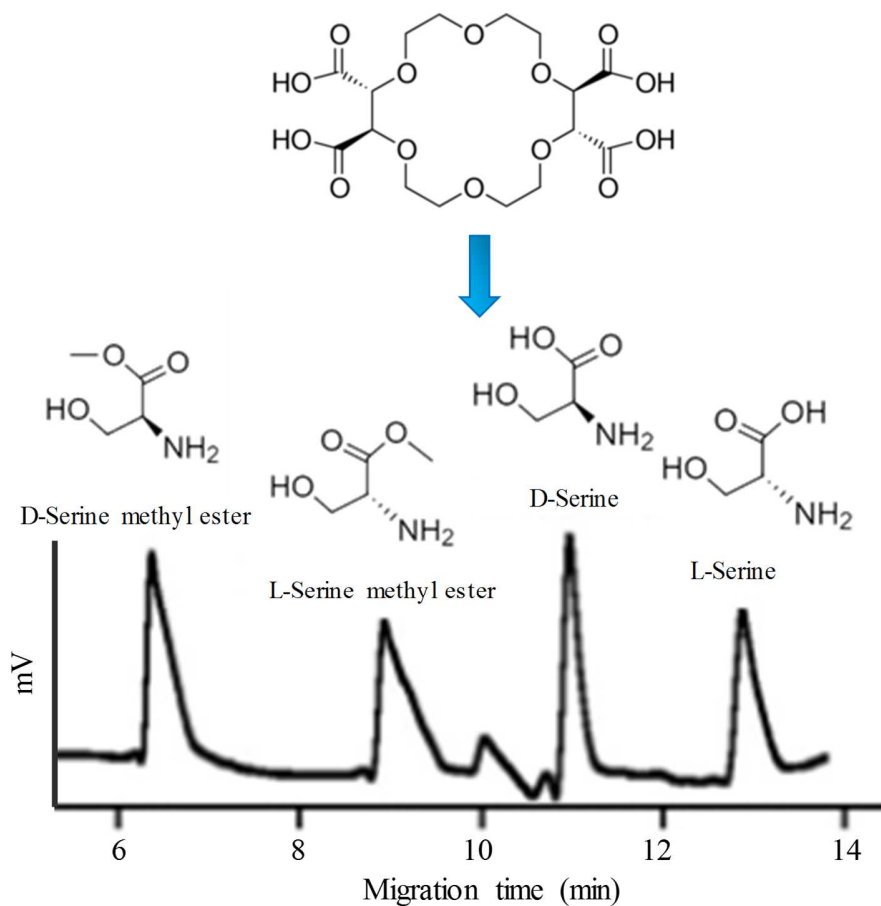


Figure 6: Electropherogram obtained for the separation of 5 mM D- and L-serine methyl esters as well as 5 mM D- and L-serine using (+)-(18-crown-6)-2,3,11,12-tetracarboxylic acid as a chiral selector and C^4D as detector. Adapted from [75]. Conditions summarized in Table 1

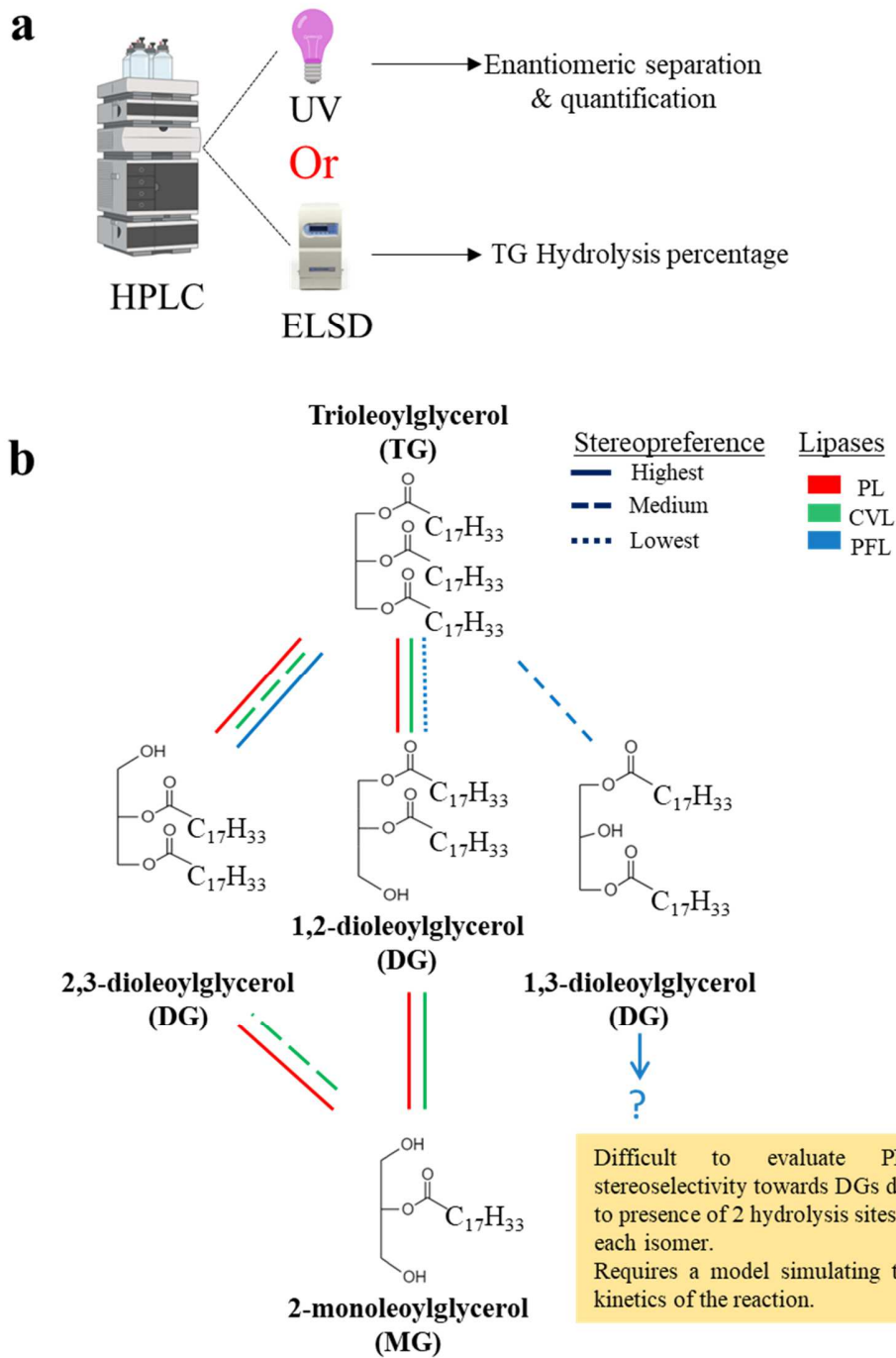
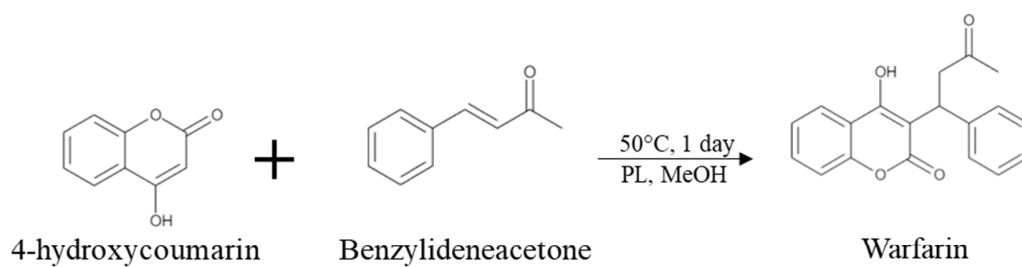


Figure 7: Quantification of enantiomeric isomers and determination of TG hydrolysis percentage by HPLC-UV and HPLC-ELSD, respectively (a) and, Stereoselectivity of three different lipases towards TG and DG enantiomers (b)

a



b

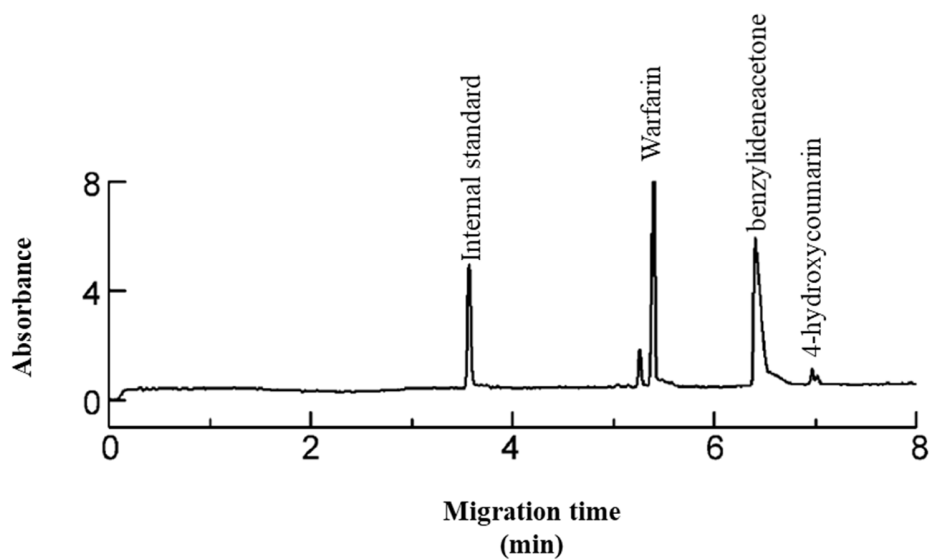
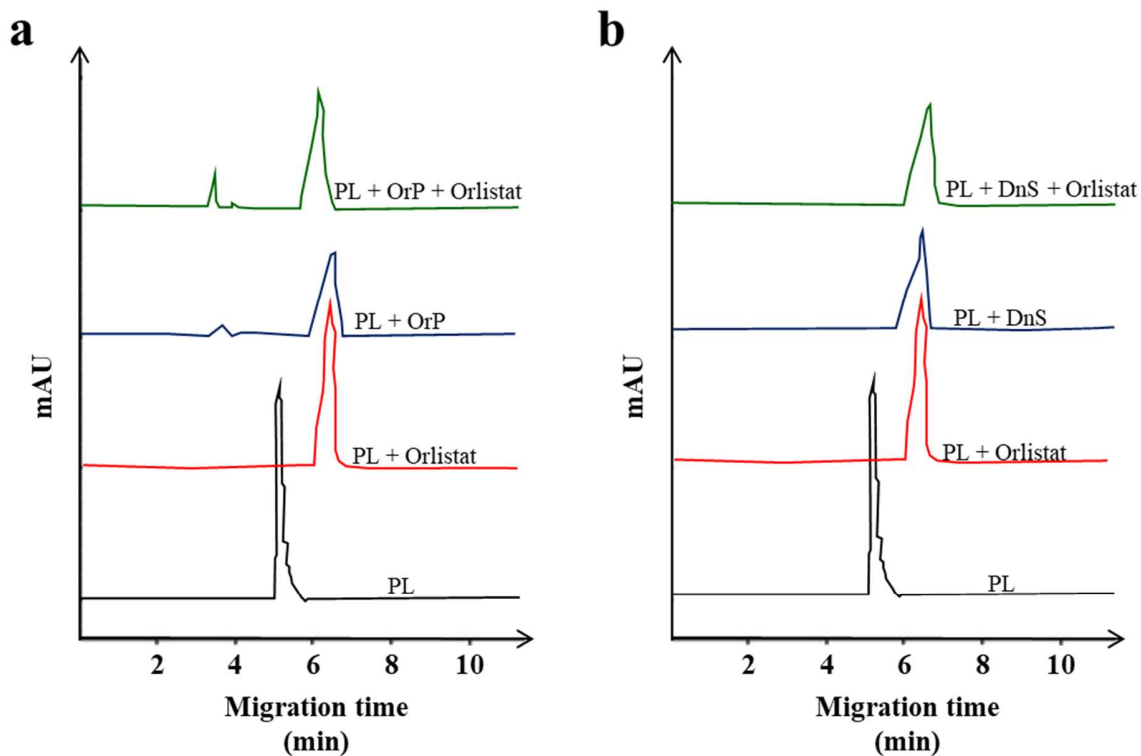


Figure 8: PL catalyzed reaction for warfarin synthesis from 4-hydroxycoumarin and benzylideneacetone (**a**) and, electropherogram of the PL-MOF reaction mixture analyzed by CE-UV at $\lambda = 214 \text{ nm}$ (**b**). Adapted from [80]. Reaction and CE conditions are summarized in Table 1



c Structures of PL inhibitor compounds

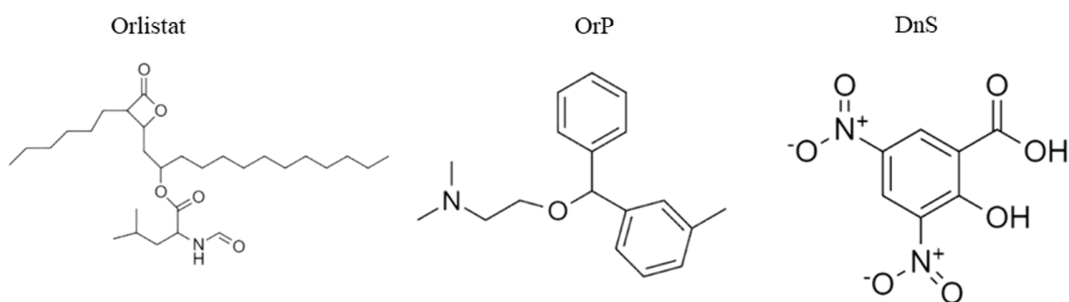


Figure 9: Electropherograms obtained for monitoring the shape of the PL peak. PL peak in the presence or absence of orlistat in addition to the presence of orphinadrine (OrP) and OrP + Orlistat (**a**) and, dinitrosalicylic acid (DnS) and DnS + Orlistat (**b**). The structures of the investigated PL inhibitory compounds are presented in (**c**). Adapted from [82]

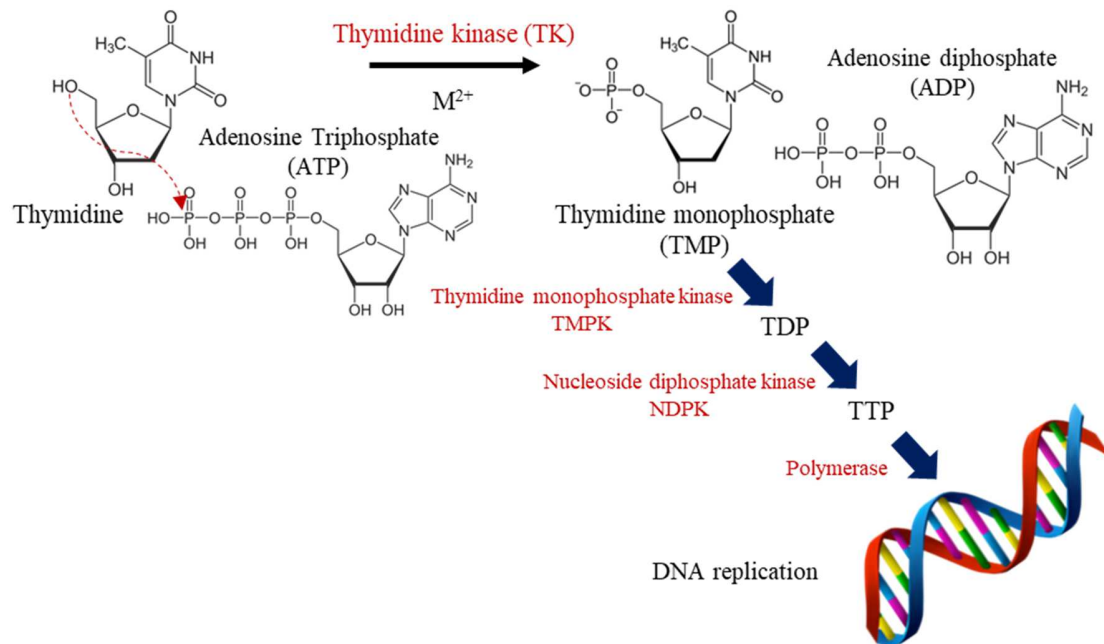


Figure 10: Illustration of the phosphorylation cascade leading to DNA replication and involving multiple kinases. M^{2+} : Divalent metal cation such as Mg^{2+} or Mn^{2+}

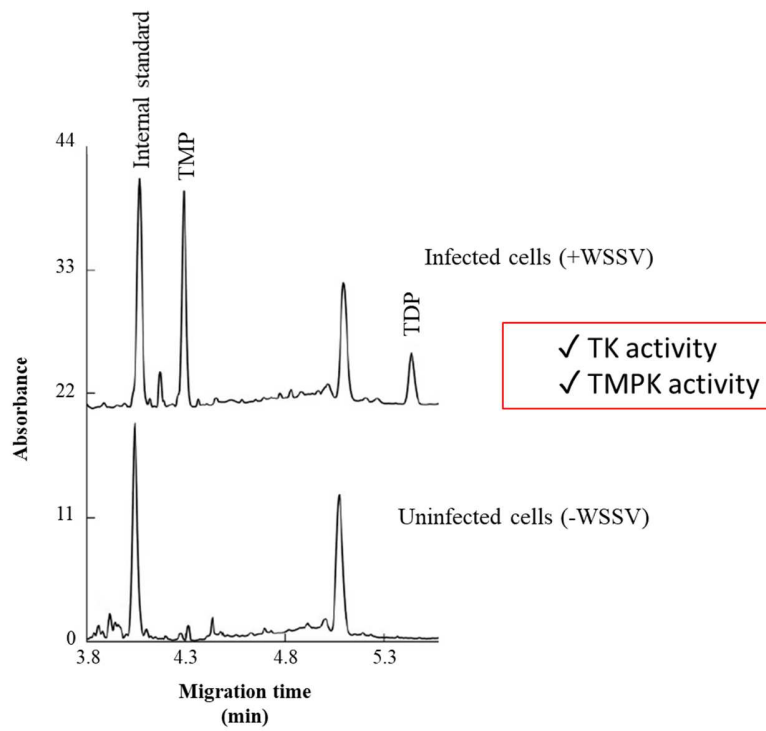


Figure 11: Electropherograms obtained for the detection of TMP and TDP from insect cell lines after infection with White spot syndrome virus (WSSV) indicating TK and TMPK activities of the virus, respectively. Adapted from [92]. Reaction and CE conditions are summarized in Table 2

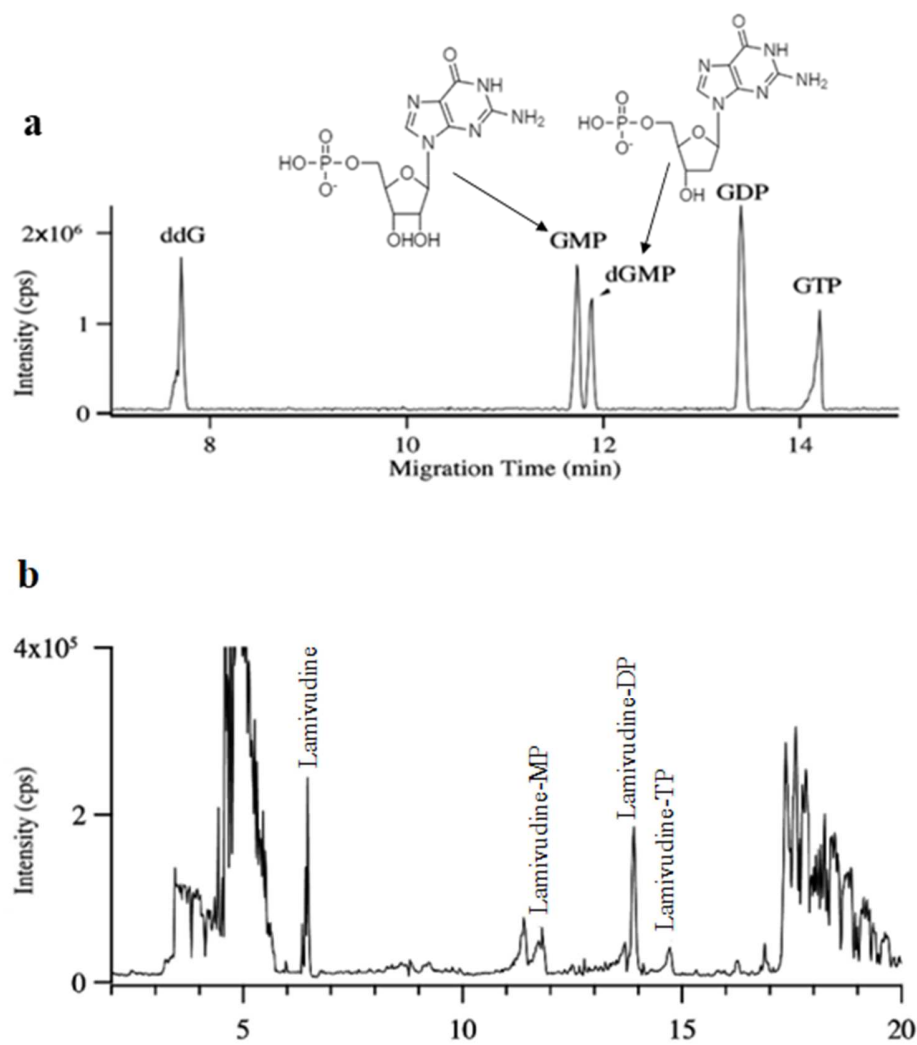


Figure 12: electropherogram representing the separation of various Guanosine nucleoside phosphates in addition to the resolution of dGMP from GMP (a) and, electropherogram of the CE-MS analysis of cell extracts incubated in lamivudine-containing medium demonstrating cellular phosphorylation activity (b). Reaction and CE-MS conditions are summarized in Table 2. Adapted from [94]

a

<u>Method A</u>	<u>Substrate</u>	<u>% phosphorylation</u>
Testing nucleoside substrates offline	Adenosine	100 ± 2
	2-Ethylaminoadenosine	3 ± 1
	2-Isopropylaminoadenosine	4 ± 0
	2-Isopropylamino-N6-isopropyladenosine	81 ± 3
	2-Benzylaminoadenosine	4 ± 0
	2-Cyclohexylaminoadenosine	3 ± 0
	2-(Pyrrolidin-1-yl)adenosine	53 ± 2
	2-(4-Benzylpiperazin-1-yl)adenosine	3 ± 0

b

<u>Method B</u>		<u>K_i value (nM)</u>				
		<u>Offline CE-UV (Method B)</u>	<u>Online-CE-UV (Method C)</u>	<u>Radioactive method</u>		
Testing AK inhibitor offline	<u>AK Inhibitor</u>	<u>Bovine AK</u>		<u>Human AK</u>		
	ABT-702	1.4 ± 0.04	1.7 ± 0.07	3.4 ± 0.03	3 ± 0.8	
<u>Method C</u>	Testing AK inhibitor online	5-IT	30.6 ± 1.7	n.d.	29 ± 6.1	26 ± 6
		A-134974	0.09 ± 0.006	0.06 ± 0.031	0.07 ± 0.006	0.06 ± 0.07

Figure 13: The percentage phosphorylation obtained for 8 substrates of bovine AK using offline CE (a) and, K_i values obtained for 3 AK inhibitors using offline and online CE as well as a conventional radioactivity assay using bovine and human AK (b). Reaction and separation conditions for all three methods are summarized in Table 2

a

Hydrodynamic injection
Uncoated Fused-silica
capillary

LOD (μM)	RSD migration time (%)
2.6 ± 0.6	2.56

Electrokinetic injection
Polyacrylamide coated
capillary

LOD (μM)	RSD migration time (%)
1.03 ± 1.4	0.53

LOD (μM)	RSD migration time (%)
0.36 ± 0.2	0.16

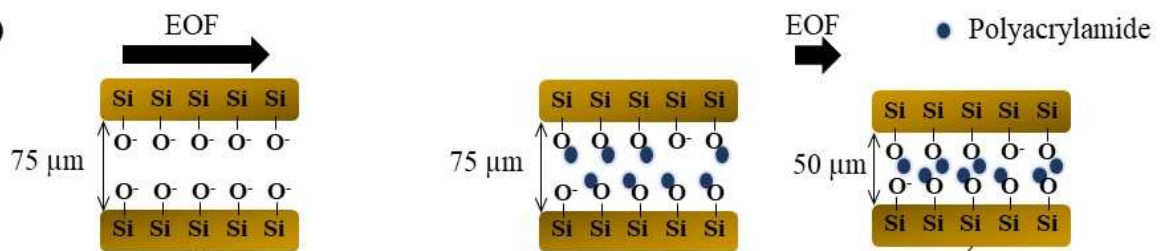
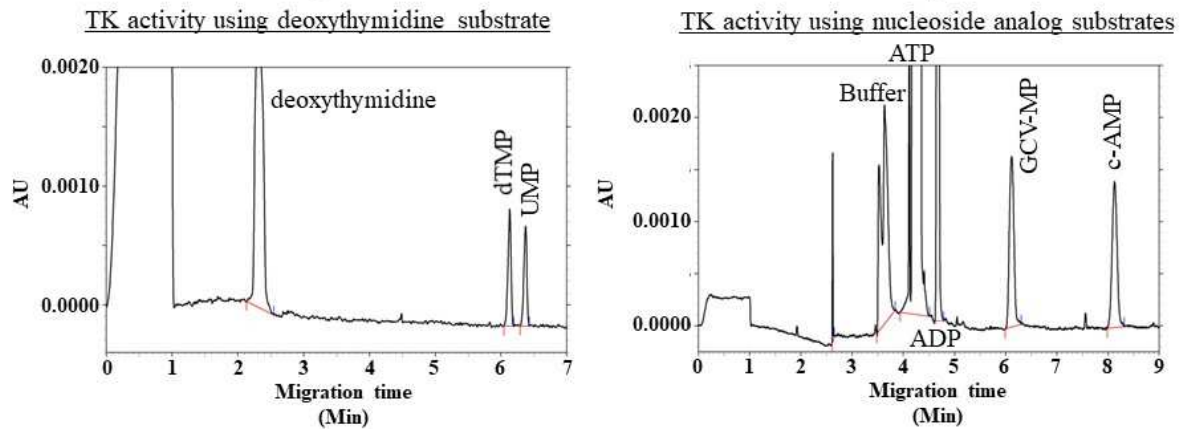
b**c**

Figure 14: The LOD of mono-phosphorylated nucleoside or nucleoside analogs and the RSD of migration times between all three types of capillaries used (a), Illustration of the inner polyacrylamide-coated surface of the capillaries (b) and, electropherograms obtained by CE-UV for the phosphorylation of endogenous deoxythymidine (left) and nucleoside analog GCV (right) (c). Conditions of enzymatic reaction and CE separation are summarized in Table 2. Electropherograms adapted from [97]

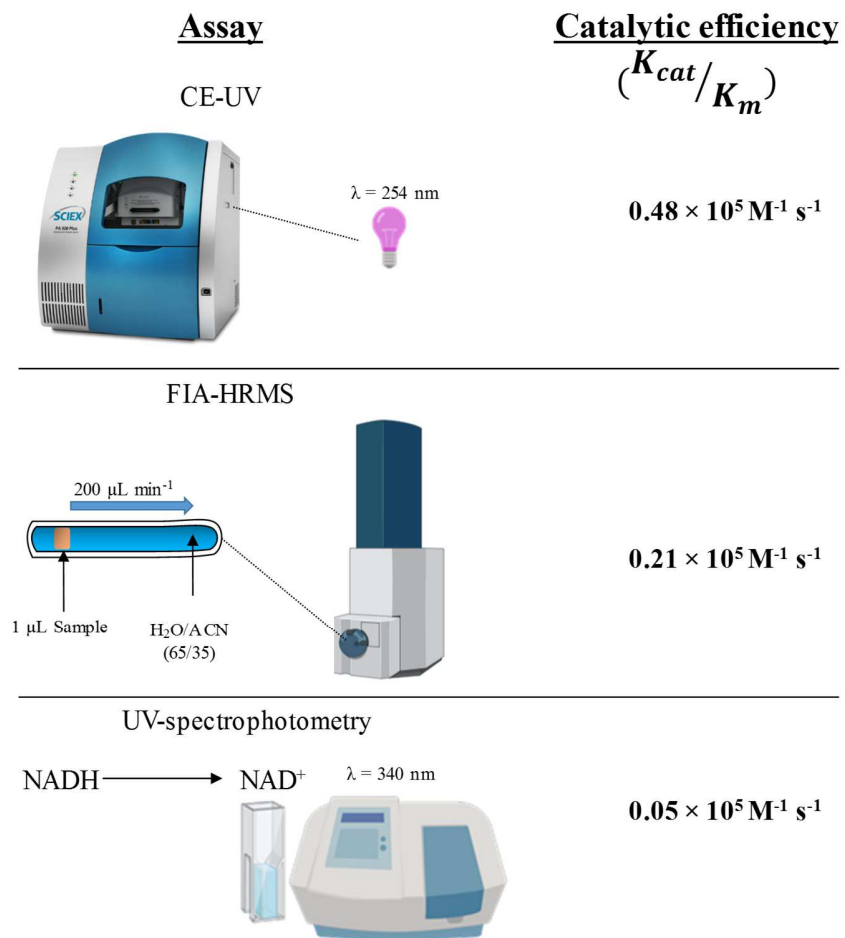


Figure 15: Catalytic efficiency of TMPK assayed by three different techniques (CE-UV, FIA-HRMS and UV spectrophotometry)

Table 1: CE-based lipase assays

Enzymatic reaction					CE separation		
Enzyme	Substrate	Inhibitor	Incubation buffer (IB)	Reaction conditions	Background electrolyte (BGE)	CE conditions	
[57]	Palastase 20000 L (Commercial lipase from <i>Rhizomucor miehei</i>)	Cream fat	-	Cream matrix, maintained at pH 7.0 through the addition of 0.1 N NaOH	<u>Offline reaction</u> Lipase added to 1000 g of cream Incubation at 40°C for 60 min with constant stirring Reaction mixture aliquoted at different time points (0-60 min). Reaction was stopped by boiling for 5 min Aliquots were mixed with tris, p-ainsate and β-CD before CE injection	20 mM Tris 10 mM p-ainsate 1 mM trimethyl β-CD (pH 8.0)	Uncoated fused-silica capillary: 80.5 cm × 50 μm i.d.; 72 cm effective length Temperature: 30°C Separation voltage: +30 kV Injection: 0.7 psi × 10 s (11 nL) Detection: indirect UV FFA at λ = 270 nm
[62]	rLipAO (lipase from <i>Aspergillus oryzae</i> fungi)	Glycerol tributyrate Or tributyrin	-	50 mM MOPS/KOH 10 mM MgCl ₂ 10 mM KCl (pH 7.2)	<u>Offline reaction:</u> Lipase added to tributyrin in IB Incubation at 37°C for 1 and 5 h Aliquots were collected and diluted with MeOH	50 mM ammonium acetate (pH 8.5)	SMILE (+) coated capillary 120 cm × 50 μm i.d. Separation voltage: -30 kV Detection: ESI-MS Butyrate ($m/z = 87.045$) Sheath liquid: 5 mM ammonium acetate in

Enzymatic reaction					CE separation	
Enzyme	Substrate	Inhibitor	Incubation buffer (IB)	Reaction conditions	Background electrolyte (BGE)	CE conditions
				to stop the reaction The sample was filtered <i>via</i> ultrafiltration with a 5,000 Da cutoff before injection into LC- or CE-MS		50% (v/v) MeOH/H ₂ O Negative ionization mode Capillary voltage: 3.5 kV Dry gas: N ₂ at 10 psi
[66]	Porcine pancreatic lipase (PL), type II Covalently immobilized onto the capillary walls <i>via</i> cross-linking	4-nitrophenyl acetate (4-NPA) Ten ethanolic plant extracts (extracted by ultrasonic-assisted extraction) used in Chinese medicines	Orlistat 10 mM Na ₂ HPO ₄ (pH 8.0) adjusted with 1 M H ₃ PO ₄	<u>Immobilized enzyme microreactor (IMER)</u> Capillary rinsed with 10 mM Na ₂ HPO ₄ for 3 min 4-NPA with or without orlistat or plant extract injected at 0.7 psi × 5 sec; 64 nL Incubation at 25°C for 4 min Reaction was stopped by the application of the separation voltage	10 mM Na ₂ HPO ₄ (pH 8.0) adjusted with 1 M H ₃ PO ₄	APTES/GA activated (16.5 cm) and uncoated fused silica (16.5 cm) capillary connected by a 0.5 cm Teflon tubing 33 cm × 75 μm i.d.; 8.5 cm effective length Temperature: 25°C Separation voltage: +15kV Injection: 0.7 psi × 5 s (64 nL) Detection: UV 4-NP at λ = 400 nm Uncoated fused-silica capillary (33 cm × 50 μm i.d.; 24.5 cm effective length)
[68]	<i>Candida rugosa</i> lipase (CRL) immobilized onto Fe ₃ O ₄ @TiO ₂ NP by electrostatic interactions.	4-nitrophenyl palmitate (4-NPP) 6 methanolic plant extracts used in Tibetan medicine	Orlistat 20 mM NaH ₂ PO ₄ (pH 4 – 10)	<u>Offline reaction</u> 4-NPP added to a solution of immobilized CRL NP	20 mM Na ₂ B ₄ O ₇ ·10H ₂ O (pH 9.0) adjusted with 1 M HCl	Temperature: 20°C

Enzymatic reaction				CE separation		
Enzyme	Substrate	Inhibitor	Incubation buffer (IB)	Reaction conditions	Background electrolyte (BGE)	CE conditions
		11 compounds isolated from <i>Oxytropis falcate</i>		For inhibition assays, plant extracts or isolated compounds were added to the mixture Incubation at 60°C for 15 min Reaction was stopped by separating immobilized CRL NP using a magnet		Separation voltage: +20 kV Detection: UV 4-NP at $\lambda = 405$ nm
[71]	Porcine pancreatic lipase (PL)	4-nitrophenyl butyrate (4-NPB)	Orlistat 7 Aqueous extracts from 3 plants (1 mg mL ⁻¹) 11 molecules purified from oakwood or wine (1 mg mL ⁻¹)	10 mM Tris 40 mM MOPS (pH 6.6)	<u>Offline reaction:</u> PL added to a solution containing: IB, Substrate Modulators (Inhibition assays) Incubation at 37°C for 5 min Reaction was stopped by boiling for 5 min Reaction mixture was centrifuged at 2000g for 5 min before CE analysis <u>Online reaction:</u> 1 st plug: PL + modulator	10 mM Tris + 40 mM MOPS (pH 6.6) Uncoated fused-silica capillary (61 cm × 50 μ m i.d.; 37 cm effective length to C ⁴ D; 51 cm effective length to UV) Temperature: 37°C Separation voltage: +30 kV Injection (offline): 0.7 psi × 5 s; (9 nL) Detection: UV 4-NP at $\lambda = 400$ nm C ⁴ D Butyrate at frequency: medium, 0 dB voltage,

Enzymatic reaction				CE separation		
Enzyme	Substrate	Inhibitor	Incubation buffer (IB)	Reaction conditions	Background electrolyte (BGE)	CE conditions
				0.5 psi × 3 s (4 nL) 2 nd plug: 4-NPB 0.5 psi × 6 s (8 nL) 3 rd plug: same as 1 st plug 4 th plug: IB 0.5 psi × 90 s (120 nL) Incubation at 37°C for 5 min Reaction was stopped as soon as the separation voltage was applied		100% gain, 010 offset, 1/3 filter frequency and 0.02 filter cut-off
[74]	<i>Candida antarctica</i> lipase B (CALB)	3-(benzyloxy)-1,1-difluoropropan-2-ol	-		22 mM NaOH + 35 mM H ₃ PO ₄ (pH 2.5) + 1.5 mM sulfobutyl ether β-cyclodextrin (β-CD)	Uncoated fused-silica capillary (40.6 cm x 50 μm; 30.2 cm effective length) 15°C +20 kV Injection: 0.1 psi x 5-10 s (1-2 nL) Detection: UV racemic substrates and products at λ = 206 nm

Enzymatic reaction					CE separation		
	Enzyme	Substrate	Inhibitor	Incubation buffer (IB)	Reaction conditions	Background electrolyte (BGE)	CE conditions
[75]	Porcine pancreatic lipase (PL)	DL-Serine methyl ester (DL-SME)	-	200 mM NaHCO ₃ (pH 7.8)	Racemic mixture of DL-SME or DL-TME in IB added to PL	2 M acetic acid + 5 mM chiral crown ether 18C6H4 [(1)-(18-(crown-6)-2,3,11,12-tetracarboxylic acid)]	Uncoated fused-silica capillary 50 cm x 50 μm i.d.; 45 cm effective length Separation voltage: +15 kV Injection: manual at 10 cm elevation for 10 s Detection: C ⁴ D DL-SME, DL-TME, DL-serine and DL-threonine
	Wheat germ lipase (WGL)	DL-Threonine methyl ester (DL-TME)			Incubation at 37°C for 2 days Aliquots taken at different time points for CE analysis		
[80]	Porcine pancreatic lipase (PL) immobilized onto 4 metal-organic frameworks (MOFs) or mesoporous silica (SBA-15)	4-hydroxycoumarin and benzylideneacetone	-	MeOH	PL (immobilized or in-solution) mixed with 1 4-hydroxycoumarin and benzylideneacetone in IB Incubation at 50°C for 1 day Centrifugation at 10K RPM for 5 min to separate the immobilized PL for recycling	132.5 mM sodium tetraborate 15 mM SDS (pH 8.5)	Uncoated fused-silica capillary 60 cm x 50 μm i.d.; 50 cm effective length Separation voltage: +28 kV Injection: 0.5 psi x 3 s (3 nL) Detection: UV Warfarin, substrates and thiourea at λ = 214 nm

Table 2: CE-based nucleoside kinase assays

Enzymatic reaction					CE separation		
	Enzyme	Substrate	Inhibitor	Incubation buffer (IB)	Reaction conditions	Background electrolyte (BGE)	CE conditions
[91]	Cytosolic 5'-nucleotidase /nucleoside phosphotransferase purified from calf thymus	Inosine	-	50 mM Tris-HCl 20 mM MgCl ₂ 1 mM dithiothreitol (DTT) pH 7.4	<u>Offline reaction:</u> A mixture of: dGMP ATP IB Inosine enzyme Incubation at 37°C for 30 min Aliquots drawn at different time intervals and mixed with cold MeOH to terminate the reaction and stored at -20°C The aliquot was centrifuged at 10000g for 15 min The supernatant was dried and then reconstituted in H ₂ O before CE analysis	50 mM NaH ₂ PO ₄ 40 mM Glycine pH 9.0 adjusted using NaOH	Uncoated fused-silica capillary 50 cm × 50 μm i.d. Temperature: 25°C Separation voltage: +20 kV Injection: 1 psi × 4 s (10 nL) Detection: UV Inosine and dGMP substrates and IMP and deoxyGuanosine products at λ = 254 nm
[92]	Thymidine kinase (TK) Thymidine monophosphate kinase (TMPK)	Thymidine and Thymidine monophosphate (TMP)	-	50 mM Tris-HCl (pH 8)	<u>Offline reaction:</u> Protein extract from insect cell lysate mixed 1:1 (v/v) with reaction solution containing: IB, Thymidine, ATP, MgCl ₂ , Bovine serum albumin, NaF,	20 mM Sodium tetraborate (pH 9.1)	Uncoated fused-silica capillary bubble cell capillary 45.5 cm × 50 μm; 37 cm effective length; 150 μm path length Temperature: 25°C Separation voltage:

Enzymatic reaction					CE separation	
Enzyme	Substrate	Inhibitor	Incubation buffer (IB)	Reaction conditions	Background electrolyte (BGE)	CE conditions
				<p>β-mercaptoethanol.</p> <p>Incubation at 37°C for 10 and 20 min The reaction was stopped by boiling for 3 min</p> <p>Reaction mixture stored at -20°C until CE analyses</p> <p>The samples were mixed with EDTA, ACN, NaCl and dAMP prior to CE injection</p>		<p>+23 kV</p> <p>Injection: 0.5 psi \times 40 s (52 nL)</p> <p>Detection: UV thymidine, dTMP and dTDP at $\lambda = 267$ nm</p>
[94]	Cellular kinases	Lamivudine	-	<p>Cell incubation media</p> <p>Confluent Hep G2 cells incubated at 37°C for 10 h in a medium containing lamivudine.</p> <p>Cells were lysed by MeOH. The cell lysates were then ultrafiltered then pre-concentrated 100-fold before CE injection.</p>	25 mM Ammonium acetate (pH 10.0)	<p>Uncoated fused-silica capillary 60 cm \times 50 μm i.d.</p> <p>Separation voltage: +15 kV</p> <p>Injection: Manual at 18 cm elevation for 30 s</p> <p>Detection: ESI-MS Lamivudine and its phosphorylated metabolites Sheath liquid: 100% MeOH at 2 μL min⁻¹ Negative ionization mode Capillary voltage: -3.6 kV Nebulizing gas flow: 0.41 L min⁻¹</p>

Enzymatic reaction					CE separation		
Enzyme	Substrate	Inhibitor	Incubation buffer (IB)	Reaction conditions	Background electrolyte (BGE)	CE conditions	
[95]	Adenosine kinase (AK) from bovine thymus	<u>Method A</u>	<u>Method A</u>	<u>Method A</u>	<u>Method A (Offline reaction)</u>	<u>Method A</u>	Dry gas flow: 1 L min ⁻¹ <u>Method A & B</u>
	Adenosine + 7 adenosine nucleoside analogs with different substituents at position 2 of the purine ring	-	20 mM Tris-HCl (pH 7.4)	AK added to the enzyme assay mixture containing: IB MgCl ₂ K ₂ HPO ₄ ATP substrate TMP internal standard	30 mM borate buffer 100 mM SDS (pH 9.5)	Uncoated fused-silica capillary 40 cm x 75 μm i.d.; 30 cm effective length	
		<u>Method B & C</u>				Temperature: 25°C	
		3 standard AK inhibitors (ABT-702, 5-IT and A-134974)	20 mM Tris-HCl (pH 7.5)	Incubation at 37°C for 15 min	<u>Method B</u> 20 mM sodium phosphate (pH 7.5)	Separation current: +95 μA	
		<u>Method B & C</u>				Injection (Offline): 0.1 psi x 25 (37.6 nL)	
	Adenosine		20 mM Tris-HCl	The reaction was stopped by boiling	<u>Method C</u>	Detection: UV AMP or nucleoside analogue monophosphate at λ = 260 nm	
			0.2 mM MgCl ₂ (pH 7.4)	Aliquots were then injected into CE.	50 mM K ₂ HPO ₄ (pH 6.5)		
				<u>Method B (Offline reaction)</u>			
				Similar to method A except: UMP internal standard Inhibitors		<u>Method C</u>	
				<u>Method C (Online reaction)</u>		Polyacrylamide-coated fused-silica capillary 30 cm x 50 μm i.d.; 20 cm effective length	
				1 st plug: IB		Temperature: 37°C	
				2 nd plug: diluted AK		Separation current: -60 μA	
				3 rd plug: Adenosine, ATP, UMP			

Enzymatic reaction				CE separation			
Enzyme	Substrate	Inhibitor	Incubation buffer (IB)	Reaction conditions	Background electrolyte (BGE)	CE conditions	
				(internal standard) and inhibitor in IB 4 th plug: IB The reaction was initiated through the application of 5 kV for 12 s Incubation at 37°C for 5 min The reaction was stopped by the application of constant current -60 μ A and the analytes were separated		Detection: UV AMP at λ = 210 nm	
[97]	Herpes simplex virus-1 (HSV-1) thymidine kinase (TK)	Thymidine Or Acyclovir (ACV) Or Ganciclovir (GCV) Or (E)-5-(2-bromovinyl)-2'-deoxyuridine (BVDU)	Acyclovir (ACV)	50 mM Tris-HCl (pH 7.4)	The reaction was initiated by adding TK to the reaction mixture previously incubated at 37°C for 2 min containing: IB ACV, GCV or BVDU ATP MgCl ₂ Thymidine (For inhibition assays) Incubation at 37°C for 15 min The reaction was stopped by boiling for 5 min The reaction mixtures were transferred to a vial containing UMP or cAMP (internal standard) before CE analysis.	50 mM dipotassium hydrogen phosphate (pH 6.5)	Polyacrylamide-coated fused-silica capillary 30 cm \times 50 μ m OR 75 μ m i.d.; 20 cm effective length Temperature: Separation current: -60 μ A Injection: -6 kV for 30 s Detection: UV TMP or monophosphorylated drug analogs at λ = 210 nm

Enzymatic reaction					CE separation		
Enzyme	Substrate	Inhibitor	Incubation buffer (IB)	Reaction conditions	Background electrolyte (BGE)	CE conditions	
[98]	Human TMPK	dTMP	-	50 mM ammonium acetate (pH 7.0)	<p>TMPK mixed with a range of dTMP concentrations in the presence of:</p> <p>IB, ATP, MgCl₂</p> <p>Incubation at 37°C for 5 min</p> <p>The reaction was stopped by boiling for 5 min</p>	80 mM ammonium acetate (pH 9.0)	<p>Uncoated fused-silica capillary (60 cm × 50 μm i.d.; 50 cm effective length)</p> <p>Temperature: 37°C</p> <p>Separation voltage: +15 kV</p> <p>Injection: 0.5 psi × 10 s (12.7 nL)</p> <p>Detection: UV dTMP and dTDP at λ = 254 nm</p>